

Observation, Analysis, and Solution: Exploring Strong Lightweight Vision Transformers via Masked Image Modeling Pre-Training

Jin Gao*, Shubo Lin*, Shaoru Wang*, Yutong Kou, Zeming Li, Liang Li, Congxuan Zhang, Xiaoqin Zhang, Yizheng Wang, and Weiming Hu, *Senior Member, IEEE*

arXiv:2404.12210v1 [cs.CV] 18 Apr 2024

Abstract—Masked image modeling (MIM) pre-training for large-scale vision transformers (ViTs) in computer vision has enabled promising downstream performance on top of the learned self-supervised ViT features. In this paper, we question if the *extremely simple* ViTs’ fine-tuning performance with a small-scale architecture can also benefit from this pre-training paradigm, which is considerably less studied yet in contrast to the well-established lightweight architecture design methodology with sophisticated components introduced. By carefully adapting various typical MIM pre-training methods to this lightweight regime and comparing them with the contrastive learning (CL) pre-training on various downstream image classification and dense prediction tasks, we systematically **observe** different behaviors between MIM and CL with respect to the downstream fine-tuning data scales. Furthermore, we **analyze** the frozen features under linear probing evaluation and also the layer representation similarities and attention maps across the obtained models, which clearly show the inferior learning of MIM pre-training on higher layers, leading to unsatisfactory fine-tuning performance on data-insufficient downstream tasks. This finding is naturally a guide to choosing appropriate distillation strategies during pre-training to **solve** the above deterioration problem. Extensive experiments on various vision tasks demonstrate the effectiveness of our observation-analysis-solution flow. In particular, our pre-training with distillation on pure lightweight ViTs with vanilla/hierarchical design (5.7M/6.5M) can achieve 79.4%/78.9% top-1 accuracy on ImageNet-1K, which is comparable to the current SOTA networks with sophisticated architecture design. It also improves the corresponding supervised pre-training baselines to achieve +2.1/+5.3 box AP and +2.0/+4.4 mask AP gains on the COCO detection and segmentation tasks. Our pre-training also enables SOTA performance on the ADE20K semantic segmentation task (42.8% mIoU) and LaSOT visual tracking task (66.1% AUC) in the lightweight regime. The latter even surpasses all the current SOTA lightweight CPU-realtime trackers.

Index Terms—Self-supervised learning, masked image modeling, vision transformers, lightweight networks, knowledge distillation.

1 INTRODUCTION

SELF-SUPERVISED learning (SSL) has shown great progress in representation learning without heavy reliance on expensive labeled data. SSL focuses on various pretext tasks for pre-training, the objectives of which provide a richer learning signal (e.g., richer visual information in computer vision field) than the supervised objective of predicting a single label or concept selected from a predefined set of different categories [1]. This can explain why several existing SSL works [1], [2], [3], [4], [5], [6] based on contrastive learning (CL) have managed to achieve comparable or even better accuracy than fully-supervised pre-training when transferring the learned representations based on ImageNet-1K [7] to downstream tasks. Prior works [8], [9], [10] have also sought to

- Jin Gao, Shubo Lin, Shaoru Wang, Yutong Kou, and Weiming Hu are with the State Key Laboratory of Multimodal Artificial Intelligence Systems, CASIA, Beijing 100190, China, and also with the School of Artificial Intelligence, University of Chinese Academy of Sciences, Beijing 101408, China. Weiming Hu is also with the School of Information Science and Technology, ShanghaiTech University, Shanghai 201210, China. Corresponding author: Shaoru Wang (wangshaoru2018@ia.ac.cn)
- Zeming Li is with the Megvii Research, Beijing 100089, China.
- Liang Li and Yizheng Wang are with the Beijing Institute of Basic Medical Sciences, Beijing 100850, China.
- Congxuan Zhang is with the Key Laboratory of Jiangxi Province for Image Processing and Pattern Recognition, Nanchang Hangkong University, Nanchang 330063, China.
- Xiaoqin Zhang is with the Key Laboratory of Intelligent Informatics for Safety & Emergency of Zhejiang Province, Wenzhou University, Wenzhou 325035, China.

* Equal contribution.

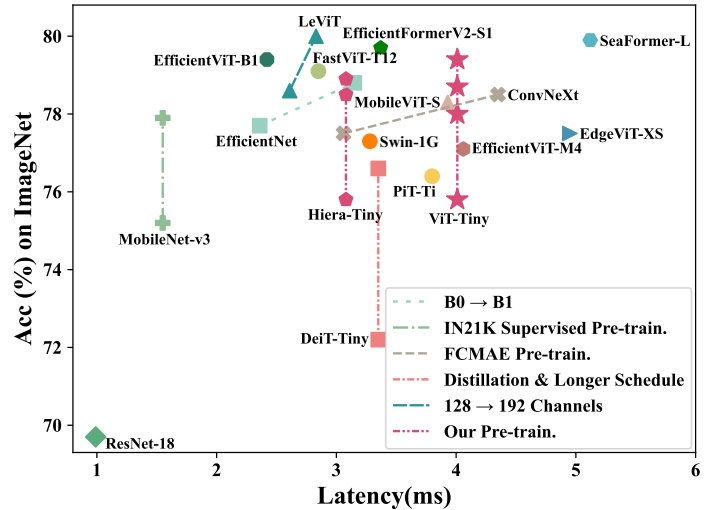


Fig. 1. Our SSL pre-training with distillation on pure lightweight ViT-Tiny (5.7M)/Hiera-Tiny (6.5M) can achieve 79.4%/78.9% top-1 accuracy on ImageNet-1K validation set, which bridges the performance gap between *extremely simple* ViT architectures and delicately designed ones in the lightweight regime. The latency is measured on Orin with batch size 1. The transfer evaluation on other downstream tasks is also impressive.

apply CL on lightweight convolutional networks (ConvNets) and improve the performance by distillation, because efficient networks are essential for modern on-device computer vision.

Recently, another SSL trend focuses on masked image modeling (MIM) pre-training (e.g., [11], [12], [13], [14]), which perfectly fits vision transformers (ViTs) [15] for vision tasks

and has shown emerging good generalization performance and scalability to large-scale models and datasets. Although supervised pre-training for ViTs can also benefit from the “LLM-like” scaling in vision, *i.e.*, scaling up training duration, model architecture size and number of training images together to improve representation quality, it has also been demonstrated that lightweight ViTs can hardly benefit from either the largest dataset or compute resources for supervised training due to the reason that their representation quality is bottlenecked by the limited capacity. In other words, the performance improvement of scaling up compute and data for supervised training of lightweight ViTs may be marginal considering the substantially increased cost of computation or collecting and labeling the data. For instance, scaling up the supervised pre-training duration on ImageNet-21K [7] (a bigger and more diverse dataset, as roughly ten times the size of ImageNet-1K) from 20 to 200 hours even for the lightweight specialized Data-efficient image Transformers (dubbed DeiT) [16] can only achieve +0.9% top-1 accuracy gain on ImageNet in our experiment. We also empirically examine whether the self-supervised pre-training on lightweight ViTs can benefit from large-scale pre-training data. A similar phenomenon to the supervised pre-training is observed that the benefit of using large-scale data is limited due to the limited capacity of lightweight ViTs. It is thus appealing to explore other factors in improving the representation quality of lightweight ViT-based models, *e.g.*, exploring the design space for ViT-based architectures or shifting from “LLM-like” scaling of data to SSL pre-training with optimized pretext objectives.

A significant body of work has been devoted to designing different lightweight ViT derivatives by introducing sophisticated components with inductive biases [17], [18], [19], [20], [21], [22], [23], [24], [25], [26], [27], leading to top-performing lightweight models, while little attention is paid to how to optimize the pre-training strategies for further improving the existing lightweight models, especially the *extremely simple* ones with plain architecture or less artificial design. We believe the latter is also of vital importance and the utilization of MIM pre-training is one of the most promising approaches which echo this direction, since MIM has achieved great progress on large-scale models. To this end, we first develop and carefully adapt various recently popular MIM pre-training methods (mainly for the large models) to the above lightweight regime, *i.e.*, the MAE [12] and SimMIM [28] methods which aim to predict raw RGB pixels of masked patches, and some methods with other pre-defined targets for prediction (*e.g.*, discrete tokens in BEiT [11] which are generated by a dVAE [29] pre-trained on DALLE [30], features from a momentum teacher in BootMAE [31], and HoG features in MaskFeat [32]). We then benchmark them along with two typical CL pre-training methods (*i.e.*, MoCo-v3 [6] and DINO [1]) and the fully-supervised pre-training methods as the baselines on ImageNet, as well as on some data-insufficient downstream classification tasks and dense prediction tasks (*e.g.*, object detection and segmentation, semantic segmentation, and visual tracking), for a closer look at the self-supervised pre-training of lightweight ViTs.

On one hand, we surprisingly find that *if proper pre-training is adopted, even the extremely simple lightweight ViTs with vanilla design show comparable performance to the current SOTA ViT derivatives with delicate design on ImageNet*. Without bells and whistles, our implementation with MIM pre-training can

achieve 78.0% top-1 accuracy (see Tab. 1) by using a slightly modified version of [16] with vanilla lightweight architecture, namely ViT-Tiny (5.7M) in this paper. This finding is intriguing since the results indicate that proper pre-training can bridge the performance gap between vanilla ViT architectures and delicately designed ones in the lightweight regime to a great extent. Although the latter ones may also enjoy high accuracy and attractive floating point operation (FLOP) counts, some of them (*e.g.*, EdgeViT-XS [23], MobileViT-S [21], MobileFormer-294M [22], SeaFormer-L [27]) with added complexity from specialized modules make the inference speed slower overall (higher latency, see Tab. 7). This interesting finding, however, does not match the practice of lightweight ViT pre-training in [33], which claims that MIM pre-training can even hurt lightweight ViT fine-tuning accuracy on ImageNet. On the other hand, we systematically observe different behaviors between MIM and CL pre-training with respect to the downstream fine-tuning data scales, *i.e.*, MIM pre-training generally outperforms CL pre-training on the data-sufficient ImageNet classification task, while *showing significantly worse performance on the data-insufficient downstream tasks*.

These findings motivate us to delve into the working mechanism of the above self-supervised pre-training methods for lightweight ViTs. More specifically, we first analyze their frozen features under linear probing evaluation and then introduce a model analysis method to study the pattern of layer behaviors during pre-training and fine-tuning, *i.e.*, analyzing the layer representation similarities across the obtained models, both of which clearly show the inferior learning of MIM pre-training on higher layers. In specific, MIM pre-training hardly learns semantics at an abstract level relevant to recognition in higher layers, which is contrary to the CL pre-training (*e.g.*, DINO [1] can automatically learn class-specific features leading to unsupervised object segmentation). This may be the reason for its unsatisfactory fine-tuning performance on data-insufficient downstream tasks. In other words, *higher layers matter in data-insufficient downstream tasks*. This is also consistent with the further model analysis by studying the attention maps across the obtained models, which shows that MIM pre-training tends to make the pre-trained models focus on local patterns with concentrated attention in higher layers. By further carefully investigating what really matters for downstream performance, however, we find that *lower layers of the pre-trained models matter more than higher ones if sufficient downstream data is provided*. We attribute it to the reason that *MIM pre-training is prone to making the attention of the downstream models more local and concentrated* than the CL pre-training and training-from-scratch settings in some layers, *i.e.*, drawing locality inductive bias from pre-training into the downstream models to make them focus on nearby image elements, which may be the key to the performance gain on the data-sufficient ImageNet classification task.

Based on the above analyses, we have developed a decoupled distillation strategy for better MIM pre-training of lightweight ViTs, which not only learns semantics at an abstract level relevant to recognition in higher layers (see Tab. 6 for the significantly improved performance on data-insufficient downstream classification tasks and dense prediction tasks), but also makes the downstream models preserve the above useful locality inductive bias (see Tab. 6 for the improved performance on the data-sufficient ImageNet classification task). We also experimentally demonstrate the effectiveness

of our observation-analysis-solution flow by exploring a simple, efficient, lightweight, yet accurate hierarchical ViT from Hiera [14], namely Hiera-Tiny (6.5M). In particular, our pre-training with distillation on the pure ViT-Tiny and Hiera-Tiny can achieve 79.4%/78.9% top-1 accuracy on ImageNet-1K, which is comparable to the current SOTA networks with sophisticated architecture design, including some high-performing lightweight ConvNets. It also improves the corresponding supervised pre-training baselines to achieve +2.1/+5.3 box AP and +2.0/+4.4 mask AP gains on the COCO detection and segmentation tasks. Our pre-training also enables SOTA performance on the ADE20K semantic segmentation task (42.8% mIoU) and LaSOT visual tracking task (66.1% AUC) in the lightweight regime. The latter even surpasses all the current SOTA lightweight CPU-realtime trackers. Our improved code and raw results are released at <https://github.com/wangsr126/mae-lite>.

2 RELATED WORK

2.1 Self-Supervised Learning

Self-supervised learning (SSL) has received considerable attention recently where a shared good representation is pre-trained for different subsequent downstream tasks without heavy reliance on expensive manual annotations. The richer learning signal in SSL pre-training enables such prior representation learning results to enjoy better transferability to various downstream tasks. This can be achieved by solving some well-designed pretext tasks, such as the pioneering works that adopt rotation prediction [34], image colorization [35], jigsaw puzzle solving [36], exemplar discrimination [37], image inpainting [38] and masked image modeling [11]. Some works also exploit automatic grouping of instances in the form of clustering [39], [40], [41], [42], [43], [44], [45], [46].

Contrastive learning (CL), as one of the discriminative approaches that follow the pioneering exemplar discrimination work, has been very popular in recent years and also achieved incredible success in improving the pre-training of various ConvNets [2], [3], [4], [5], [47], [48], [49], [50] and ViTs [1], [6]. Concretely, by defining different loss functions, CL pre-training aims to push the representations of different views of the same image (positive pairs) towards each other in the embedding space while the representations of views from different images (negative pairs) are pulled against each other, or even without explicitly discriminating between negative pairs from different images. It relies on different data augmentation strategies to augment the different views. Several other earlier works also explore to match the bag-of-visual-words representations [51] or train features to align to the targets that are sampled from an uninformative noise distribution [52]. Recently, some works [8], [9], [10] have sought to apply CL on lightweight ConvNets and improve the performance by distillation.

Masked image modeling (MIM) with a broad spectrum of design choices, from framework designs [12], [28], [31], [53], [54] to mask strategy [55], [56], [57], [58], [59] and prediction target [11], [13], [32], [60], [61], [62] designs, has drawn much attention of the vision community. It takes a similar formulation to masked language modeling (MLM) in BERT [63], *i.e.*, learning by recovering the masked patches/tokens from the visible ones in the corrupted image. For instance, BEiT [11] is the pioneer along this line which predicts masked tokens generated by a discrete VAE [29]

pre-trained on DALLE [30]. MAE [12], SimMIM [28], and BootMAE [31] all use RGB pixels as the reconstruction target for groundtruth while they adopt different special designs on the architecture of prediction head. For better supervisions, iBot [13], data2vec [60], and BootMAE [31] innovatively reconstruct the masked tokens with the online tokenizer outputs of EMA (exponential moving average) updated models as supervision; MaskFeat [32] reveals that simple histogram of oriented gradients as in HOG descriptor is a particularly effective target for continuous feature regression; the pre-trained teachers obtained from DINO [1] and CLIP [64] are also exploited in some works [32], [55], [62], [65]. It has been demonstrated that these methods can scale up well on large ViTs, while their performance on lightweight ones is seldom investigated. Some works [11], [28], [66], [67] also explore the alternative MIM frameworks for use with ConvNets.

In this paper, we develop and carefully adapt various recently popular MIM pre-training methods to the lightweight regime of ViTs, and also comprehensively benchmark them along with two typical CL pre-training methods and the fully-supervised pre-training methods as the baselines, so as to explore strong lightweight ViTs through MIM pre-training.

2.2 Vision Transformers

Vision transformers (ViTs) [15] is the pioneering work that applies a transformer architecture (a stack of attention modules [68]) on image patches and shows very competitive results by introducing mean color as prediction targets. Without using any convolution to have an inductive bias¹ [69] to focus on spatially neighbor image elements/tokens, this preliminary attempt requires a large and curated dataset to regularize the training and make the learned transformer effective. Recently, the performance of ViTs has been largely improved thanks to better training recipes [16], [70], [71]. For instance, DeiT in [16] introduces a ConvNet teacher to help the supervised training of the ViT student with vanilla architecture to acquire some inductive biases. Besides, better architecture design is explored in some ViT derivatives [18], [20] which focus on improving self-attention mechanism to boost performance. For instance, CaiT [20] introduces the LayerScale and class-attention designs for going deeper with ViTs while XcIT [18] replaces the self attention with a novel cross-covariance attention for reducing the quadratic complexity of self attention to linear complexity.

Hybrid architecture design has gained popularity recently with the emergence of ViTs because it can explicitly incorporate necessary inductive biases for ViT-based architectures. ConvNets have benefited from years of manual (*e.g.*, [66], [72], [73], [74], [75], [76], [77], [78], [79], [80]) and automated (*e.g.*, [81], [82], [83], [84], [85]) network designs, with some of them focusing on finding a good trade-off between computational efficiency (*i.e.*, fewer parameters and lower latency) and accuracy, *e.g.*, the families of RegNet [79], EfficientNet [81], MobileNet [76], [82], ConvNeXt [66], [80], *etc.* In specific, the ConvNeXt family [66], [80] modernizes the ResNet [74] architecture following the ViT design choices. Inspired by the success of these ConvNets, hybrid architecture design for various ViT derivatives explores to restrict the attention region

1. Different inductive biases can be injected into different learning algorithms through architectural choices, the objective function, the curriculum, or the optimization regime.

to nearby tokens [86], [87] or aggregate the neighboring tokens for progressively reduced token numbers [19], [88], [89]. Many other hybrid works [17], [21], [22], [23], [24], [25], [90], [91], [92], [93], [94], [95], [96], [97] are also inspired by investigating the combination of ConvNets and ViTs. The merit behind this integration is that it can capture both long range dependencies using self-attention mechanism of ViTs and local information using local kernels in ConvNets, and then make a fusion to improve performance on vision tasks.

Lightweight models are friendly to resource-constrained devices, so most of the above ViT derivatives have either provided their corresponding lightweight versions or been specifically designed for a better efficiency-accuracy trade-off. For example, the lightweight regime of Mobile-Former [22] covers the computational cost range from 26 MFLOPs to 508 MFLOPs. For LeViT [17], it covers the parameter number range from 7.8 M to 39.1 M. Although Mobile-Former has relatively fewer network parameters and costs significantly fewer FLOPs than LeViT, the latter enjoys much higher inference speed thanks to the ConvNet’s clothing design without using too many complicated operators. By getting rid of the complex trade-offs among model size (or parameter number), FLOPs, inference speed (or latency), and accuracy of the above ViT derivatives with delicate design, a preliminary version of this paper published in ICML’23 [98] is the first to systematically study the effects of applying SSL pre-training on lightweight ViTs with vanilla architecture design. It is demonstrated that proper pre-training based on the proposed distillation strategy can even close the performance gap between vanilla ViT architectures and delicately designed ones in the lightweight regime to a great extent. The present work goes further to investigate more typical MIM pre-training methods to provide more comprehensive analyses, propose an improved decoupled distillation strategy to unleash the great potential of pre-training, and provide more experimental results to make the conclusion more convincing. The new results especially on the downstream semantic segmentation and visual tracking tasks and using another *extremely simple* lightweight hierarchical ViT as the experimental unit are also impressive.

2.3 Knowledge Distillation

Knowledge distillation (KD), a mainstream approach for model compression [99], [100], [101], is best known as an effective method for taking advantage of a large number of parameters in a teacher model during training, while having an optimized smaller and efficient student model during inference. Beyond model compression, KD is also reckoned to be able to combine strengths of different learning algorithms [69] by transferring the effect of inductive biases between different models. It is claimed that having the right inductive biases is essential for obtaining high performance when data or compute is a limiting factor. For instance, the distillation-based supervised training (or fine-tuning) in DeiT [16] achieves better accuracy on vanilla ViTs by adopting a ConvNet as the teacher. Extensive methodologies have also been proposed to improve the distilling effectiveness. In [100], the mimic error of a small student network towards the soft logit output of a larger teacher network is adopted to guide the transferring of the knowledge. FitNet [101] proposes to distill semantic information from intermediate features, and a mean-square-error-based hint loss is adopted. Besides, the

channel attention [102] and the relation of examples [103] are considered as the learned knowledge to be transferred. Moreover, KD is widely adopted in various tasks apart from classification tasks, *e.g.*, object detection [104] and semantic segmentation [105].

Under self-supervised settings, there have been a few works performing KD technologies to transfer knowledge from a larger pre-trained teacher to a lightweight student model for better representations, because the naive SSL methods do not work well for lightweight models as shown in [8]. For instance, some works [106], [107], [108], [109] attend to distill large-scale pre-trained language models. In the area of computer vision, CompRes [9] and SEED [8] employ knowledge distillation to improve the self-supervised visual representation learning capability of small ConvNet models, relying on a CL-based MoCo [3] framework. A more flexible framework based on CL is proposed in DisCo [110] to transfer ConvNet teachers’ knowledge to smaller students. In [111], a simple feature distillation method is proposed to improve the fine-tuning performance of ViTs based on various pre-training methods, including CL-based approaches such as DINO [1] and EsViT [112], visual-language pre-trained models such as CLIP [64], and supervised models such as DeiT [16]. Some methods also adopt online distillation [10], [113], which recommends training the teachers and students at the same time and conducting SSL and KD simultaneously. Others focus on taking some inspiration from SSL to boost the performance of task-specific distillation under a fully supervised setting. For example, CRD [114] introduces a new contrastive loss between teacher and student networks for better knowledge distillation. In SSKD [115], SSL is treated as an auxiliary task to help extract richer knowledge from a teacher network.

In this paper, we focus on further improving the performance of MIM pre-trained lightweight ViTs by distillation, which is developed following the guidance of our thorough analyses. Our MIM pre-training with distillation not only helps the pre-trained lightweight ViTs to learn semantics at an abstract level relevant to recognition in higher layers, but also makes the downstream models preserve the useful locality inductive bias benefiting from MIM pre-training. Although our distillation bears some similarities to the recent TinyMIM work [33], the whole of our observation-analysis-solution flow is orthogonal to it as it aims to systematically study the distillation framework for MIM pre-trained ViTs.

3 OBSERVATION

In this section, we carefully adapt various typical pre-training methods to the lightweight regime of pre-training ViTs, benchmark the pre-trained models with a small-scale architecture on ImageNet, and further evaluate their transferability to other datasets and tasks, which addresses a little-explored question: how well does pre-training work on lightweight ViTs with vanilla architecture design, especially for MIM pre-training?

3.1 Preliminaries and Experimental Study Design

Experimental Unit. We use a slightly modified version of [16] with vanilla lightweight architecture, namely ViT-Tiny, as the experimental unit in our study, which contains 5.7M parameters. We examine the effect of different pre-training methods on it by benchmarking the corresponding

downstream performance. Following [16], it consists of one patch embedding layer and twelve transformer blocks with the embedding dimension set to 192. The fixed-size input RGB image at resolution 224×224 is decomposed into a batch of patches of a fixed size of 16×16 pixels. *We slightly modify the number of heads from 3 to 12 as we find this can improve the model’s expressive power.* We choose ViT-Tiny for study because its non-hybrid vanilla architecture has no strong inductive biases by design and its simplicity² allows us to focus more directly on the impact of pre-training. In addition, ViT-Tiny is an ideal experimental unit on which almost all existing pre-training methods can be directly applied.

Evaluation Protocols. *Linear probing* has been a standard evaluation protocol to compare the quality of the pre-trained weights [2], [3], [4], [5], in which only the prediction head is tuned based on the downstream training set while the pre-trained representations are kept frozen. However, prior works point out that linear evaluation does not always correlate with the practical utility [12], [121]. In this study, we mainly adopt *fine-tuning* as the default evaluation protocol to benchmark the downstream performance, in which all the layers are tuned by initializing them with the pre-trained models. We leave the *linear probing* evaluation for analysis in Sec. 4 to investigate the secrets behind pre-training. By default, we do the *fine-tuning* evaluation on ImageNet [7] by tuning the whole models on its training set and then evaluating them on the validation set. Several other downstream classification tasks, object detection and segmentation tasks, semantic segmentation task, and single object tracking task are also exploited for comparison.

Compared Methods. We develop and carefully adapt various recently popular MIM pre-training methods (mainly for the large models) to apply them on ViT-Tiny, *i.e.*, the MAE [12] and SimMIM [28] methods which aim to predict raw RGB pixels of masked patches, and some methods with other pre-defined targets for prediction (*e.g.*, discrete tokens in BEiT [11], features from a momentum teacher in BootMAE [2], and HoG features in MaskFeat [72]). We also benchmark them along with two typical CL pre-training methods (*i.e.*, MoCo-v3 [6] and DINO [1]) and the fully-supervised pre-training methods as the baselines.

Baseline without pre-training. Largely following the recipe in [16], we train a ViT-Tiny model from scratch for 300 epochs on the training set of ImageNet-1K (dubbed IN1K), which serves as the baseline without pre-training in our study. It achieves 74.5% top-1 accuracy on the validation set of IN1K, surpassing that achieved based on the original architecture with 3 heads (*i.e.*, 72.2% in [16]). It further reaches 75.8% by adopting our improved training recipe with some optimized hyper-parameters for augmentations (*i.e.*, weaker regularization and augmentation than training large-scale models). Besides, layer-wise *lr* decay is also taken into consideration during *fine-tuning* following [11], [12]. Please refer to Sec. A.1 for more details. This can be seen as a strong baseline to examine the pre-training in our study because it even surpasses the original transformer-specific distillation-based version in [16] (*i.e.*, 74.5%).

Supervised pre-training baselines. In [70], a comprehensive study of the trade-offs between model regularization, data augmentation, training data size and compute budget in ViTs

is conducted. It is evident that the increased compute and AugReg (*i.e.*, a combination of modern data augmentation and model regularization techniques) can yield significantly better performance than the plain pre-training on the training set of ImageNet-21K (dubbed IN21K). So we follow the supervised pre-training recipe in [70] and scale up the pre-training duration on IN21K from 30 to 300 epochs to serve as our supervised pre-training baselines.

CL pre-training baselines. To adapt MoCo-v3 [6] and DINO [1] to ViT-Tiny, we re-implement them with ViT-Tiny as encoder and largely follow the original setups in their papers. We conduct 400-epoch pre-training on IN1K for them. In [6], it is claimed that instability is a major issue that impacts self-supervised ViT pre-training and causes mild degradation in accuracy, and a simple trick by adopting fixed random patch projection (the first layer of a ViT model) is proposed to improve the stability in practice. However, we find that instability is not the main issue for MoCo-v3 adaptation to ViT-Tiny in our study, and higher performance is achieved with a learned patch projection layer. In [1], DINO is interpreted as a form of knowledge distillation with **no** labels, where a centering and sharpening of the teacher output is used to avoid collapse.

MIM pre-training methods. We carefully adapt MIM MAE [12], BEiT [11], BootMAE [31] and MaskFeat [32] to ViT-Tiny by investigating the different effects of several basic factors and components in their frameworks. For instance, as a key component, decoder determines the semantic level of the learned latent representations. It has been validated that MIM works well across a wide range of the decoder’s width and depth under the *fine-tuning protocol* when the encoder is large. However, we experimentally find that MIM prefers a much more lightweight decoder when the encoder is altered to ViT-Tiny, *i.e.*, a decoder consisting of one transformer block with the head number and width set to 3 and 96. We also conduct a small sweep over 5 masking ratios {0.45, 0.55, 0.65, 0.75, 0.85} and find that 0.75 achieves the best performance. Other setups in the above papers remain intact including the optimizer, learning rate, batch size, argumentation, *etc.* As for SimMIM [28] adaptation to ViT-Tiny, we rigorously follow the original settings in the paper. We also do MIM pre-training on IN1K for 400 epochs.

3.2 Fine-Tuning Evaluation on ImageNet Classification

Fine-Tuning Evaluation. We follow the practice of supervised ViT-Tiny training with our improved recipe in Sec. A.1 for *fine-tuning* evaluation, though the decay coefficient in the layer-wise *lr* decay schedule is separately optimized for different pre-trained models. Besides, we use global average pooling (GAP) after the final block during the *fine-tuning* of both the MIM and CL pre-trained models, which is, however, not the common practice for MoCo-v3 [6]. We adopt GAP for MoCo-v3 as it significantly helps to surpass the model using the original configuration based on a class token (76.8% *vs.* 73.7%) for our used lightweight ViT-Tiny.

Observation 1. As shown in Tab. 1, almost all of the compared pre-training methods, including both the fully-supervised and self-supervised ones, can achieve better downstream fine-tuning performance on the ImageNet classification task than the random initialization paradigm without pre-training, whilst *MIM pre-training with moderate pre-training cost consumed*

2. In this section, we also do not use some recent techniques like relative position bias [17], [86], [116], [117], [118], [119], [120] and LayerScale [20].

TABLE 1

Comparison Across Different Pre-Training Methods by Evaluating the Pre-Trained Models on Data-Sufficient IN1K. We Report Top-1 Accuracy on Its Validation Set. Our Modified ViT-Tiny with Vanilla Architecture Is Used As the Experimental Unit. The Pre-Training Time Is Measured on an $8\times V100$ GPU Machine. ‘Ori.’ Represents the Original Training/Fine-Tuning Recipe in DeiT [16] and ‘Ours’ Represents Our Improved Recipe Over It (See Sec. A.1).

Models	Pre-Training				Fine-Tuning			Top-1 Acc. (%)
	Methods	Data	#Epochs	Time (h)	Recipe	Distill.	#Epochs	
<i>MIM Self-Supervised</i>								
	MAE [12]	IN1K w/o labels	400	23	Ours	✗	300	78.0
	SimMIM [28]	IN1K w/o labels	400	40	Ours	✗	300	77.9
	BEiT [11]	IN1K w/o labels	400	59	Ours	✗	300	77.7
	BootMAE [31]	IN1K w/o labels	400	30	Ours	✗	300	77.9
	MaskFeat [32]	IN1K w/o labels	400	34	Ours	✗	300	77.9
<i>Vanilla Architecture</i>								
<i>CL Self-Supervised</i>								
ViT-Tiny (5.7M)	DINO [1]	IN1K w/o labels	400	83	Ours	✗	300	77.2
	MoCo-v3 [6]	IN1K w/o labels	400	52	Ours	✗	300	76.8
<i>Supervised</i>								
	AugReg [70]	IN21K w/ labels	300	200	Ours	✗	300	77.8
	AugReg [70]	IN21K w/ labels	30	20	Ours	✗	300	76.9
	Our Recipe	IN1K w/ labels	300	20	Ours	✗	300	76.5
<i>W/O Pre-Training</i>								
	Random Init. [16]	-	-	0	Ours	✗	300	75.8
	Random Init. [16]	-	-	0	Ori.	✗	300	74.5

outperforms the compared pre-training baselines. As we scale up the supervised pre-training duration on IN21K from 30 to 300 epochs, we find that the $10\times$ longer schedule can achieve a comparable performance (*i.e.*, 77.8%) to the MIM pre-training, while the pre-training cost gets much higher due to the significantly increased pre-training time, let alone the used expensive labels. We also conduct the supervised pre-training with 300 epochs on IN1K using our fine-tuning recipe to better show the benefits of self-supervised pre-training or increasing the training data size. All the results indicate that the *extremely simple* lightweight ViTs with vanilla design have great potential which can be unleashed via proper pre-training.

Observation 2. The above observation encourages us to further explore how the enhanced lightweight ViTs perform in comparison to the recent SOTA lightweight ViT derivatives (including both the hybrid and non-hybrid) as introduced in Tab. 7. It can be observed that *the enhanced vanilla ViT-Tiny through MIM pre-training can also achieve SOTA performance on par with some superior ViT derivatives with comparable parameter number.* It is noteworthy that these delicately designed architectures in the lightweight regime, despite lack of pre-training, achieve top performance on the ImageNet classification task by seeking to (1) extend the supervised fine-tuning duration to a much longer schedule (*e.g.*, 1000 epochs in LeViT [17] and PiT [19]), (2) introduce distillation-driven training to regularize the fine-tuning (*e.g.*, in LeViT [17], XCiT [18], PiT [19], and CaiT [20], *etc.*), or (3) use some recent techniques like relative position bias [116], [117], [118], [119], [120] (*e.g.*, in LeViT [17] and Swin [86]), conditional positional encoding [122] (*e.g.*, in EdgeViT [23]) and LayerScale (*e.g.*, in XCiT [18]). The competing results of the enhanced vanilla ViT-Tiny demonstrate the benefits of studying MIM pre-training on *extremely simple* lightweight ViTs, which may be orthogonal to the network architecture design methodology in the ViT derivatives. Besides, *extremely simple* architectures are usually friendly to the real-world deployment by getting rid of the

complicated modules existing in some ViT derivatives (*e.g.*, EdgeViT-XS [23], MobileViT-S [21], MobileFormer-294M [22], SeaFormer-L [27]).

Observation 3. We also empirically examine whether the self-supervised pre-training on lightweight ViTs can benefit from large-scale pre-training data. In Tab. 2, we study the effect of varying the pre-training data size and class distribution with two typical SSL methods (*i.e.*, MoCo-v3 and MAE) applied on ViT-Tiny. We first consider the much larger dataset IN21K, however, few improvements are observed for both MoCo-v3 and MAE. We believe the limited capacity of *extremely simple* lightweight ViTs also bottlenecks the representation quality of self-supervised pre-training even with the “LLM-like” scaling of data. We further consider two subsets of IN1K containing 10% and 1% of the total examples (IN1K 10% and IN1K 1%) balanced in terms of classes [123] and one subset with long-tailed class distribution [124] (IN1K-LT). Surprisingly, MAE pre-training has marginal performance declines on these subsets, showing more robustness than MoCo-v3 in terms of the pre-training data size and class distribution.

3.3 Transfer Learning Evaluation on Downstream Tasks

We further examine the transfer learning performance of the pre-trained models in Tab. 3. We only consider the models pre-trained based on IN1K for simplicity, involving their transfer performance on some other downstream classification tasks and dense prediction tasks.

For the classification tasks, we investigate the performance on the relatively smaller datasets than IN1K to question if the pre-trained models transfer well on these data-insufficient tasks, including Flowers-102 [125] (Flowers for short), Oxford-IIIT Pets [126] (Pets), FGVC-Aircraft [127] (Aircraft), Stanford Cars [128] (Cars), CIFAR100 [129], iNaturalist 2018 [130] (iNat18). For all these datasets except iNat18, we conduct a small sweep for some key fine-tuning parameters, *i.e.*, the learning rate, training epoch number and layer-wise *lr*

TABLE 2

Effect of Varying the SSL Pre-Training Data Size and Class Distribution Based on ViT-Tiny. We Follow the 400-Epcho Self-Supervised Pre-Train, 300-Epoch Supervised Fine-Tune Paradigm. Top-1 Accuracy on the Validation Set of IN1K Is Reported.

Methods \ Datasets	IN1K 100%	IN1K 10%	IN1K 1%	IN1K-LT	IN21K
MoCo-v3 [6]	76.8	76.5 (-0.3)	76.2 (-0.6)	76.1 (-0.7)	76.9 (+0.1)
MAE [12]	78.0	78.0 (+0.0)	77.9 (-0.1)	77.9 (-0.1)	78.0 (+0.0)

TABLE 3

Transfer Evaluation of Our Modified ViT-Tiny on Some Data-Insufficient Downstream Classification Tasks and Dense Prediction Tasks. Top-1 Accuracy Is Reported for Classification Tasks, mIoU Is for ADE20K Segmentation, AUC Is for LaSOT Tracking, and AP Is for COCO Detection (Det.) and Segmentation (Seg.). The Dataset Scale Is Represented As (Train-Size Per Epoch/#Train-Classes).

Methods \ Datasets	Downstream Classification Tasks						Downstream Dense Prediction Tasks		
	Flowers (2k/102)	Pets (4k/37)	Aircraft (7k/100)	Cars (8k/196)	CIFAR100 (50k/100)	iNat18 (438k/8142)	ADE20K (20k/150)	LaSOT (60k/201)	COCO (det./seg.) (118k/80)
W/O Pre-Training	30.2	26.1	9.4	6.8	42.7	57.1	21.3	56.1	32.7/28.9
<i>Supervised (IN1K)</i>									
Our Recipe	96.4	93.1	73.5	85.6	85.8	64.7	41.5	64.1	40.4/35.5
<i>CL Self-Supervised</i>									
DINO [1]	95.6	89.3	73.6	84.5	84.7	64.7	39.8	64.3	41.4/36.7
MoCo-v3 [6]	94.8	87.8	73.7	83.9	83.9	63.7	38.1	62.9	39.7/35.1
<i>MIM Self-Supervised</i>									
MaskFeat [32]	92.2	85.5	72.9	82.4	82.6	64.2	38.1	63.8	41.4/36.5
BootMAE [31]	89.4	79.6	69.8	79.4	80.0	63.6	36.4	63.4	39.9/35.4
BEiT [11]	89.2	78.9	65.8	77.6	79.2	63.2	35.7	62.1	39.1/34.7
MAE [12]	85.8	76.5	64.6	78.8	78.9	64.0	34.5	61.6	39.9/35.4
SimMIM [28]	77.2	68.9	55.9	70.4	77.7	63.8	35.5	63.4	39.3/34.8

decay coefficient, to achieve the optimal fine-tuning results on these datasets (see Sec. A.2 for more details). Besides, we adopt random resized crop and random horizontal flipping as the augmentations and do not use any regularization (*e.g.*, weight decay, dropout, or the stochastic depth regularization technique [131]). For iNat18, we follow the same training configurations to those on ImageNet (see Sec. A.1).

For the dense prediction tasks, we mainly consider the object detection and segmentation tasks on COCO [132], semantic segmentation task on ADE20K [133], and visual tracking task on LaSOT [134]. For the tasks on COCO, we reproduce and rigorously follow the setup in [135], except replacing the backbone with ViT-Tiny and decreasing the input image size from 1024 to 640 to make it trainable on a single machine with 8 NVIDIA V100s like other lightweight detectors. We fine-tune for up to 100 epochs with different pre-trained models as the initialization of the backbone. We do not use layer-wise lr decay since we find it useless for the tiny backbone on these COCO tasks. The weight decay is 0.05 and the stochastic depth regularization [131] is not used. For the semantic segmentation task, we reproduce the same setup in MAE [12] and adopt UperNet framework [136] for evaluation, which follows the semantic segmentation code of [11]. In our reproduction, we only replace the backbone encoder with different pre-trained ViT-Tiny models as the initialization and keep the decoder (several deconvolution layers) intact. The input image size is 512×512 . For the tracking task, we experiment on the large-scale dataset LaSOT [134] using a recent strong baseline tracker OTrack [137]. We reproduce the setup of speed-oriented version of OTrack with input image resolution set to 256×256 and only replace the backbone, which is responsible for joint feature extraction and relation modeling, with ViT-Tiny and use different pre-trained ViT-Tiny models as the initialization.

Observation 4. As shown in Tab. 3, we first find it hard to achieve promising transfer evaluation results for our modified

ViT-Tiny on the evaluated downstream tasks by training from scratch without any pre-training. The results significantly lag behind those models that adopt various pre-training. Second, despite that using various pre-training methods shows better performance, the relative superiority and inferiority comparisons between these pre-training methods exhibit distinct characteristics from those on ImageNet (see Tab. 1). We find that *downstream data scale matters* during transfer learning. The MIM-based pre-training approaches tend to achieve downstream performance inferior to the fully-supervised counterpart, while the performance gap is narrowed more or less as the data scale of the downstream task increases. Moreover, MIM-based pre-training even shows inferior results to CL-based approaches. We conjecture that it is due to their different layer behaviors during pre-training and fine-tuning as discussed in detail in the following section.

4 ANALYSIS

In this section, we introduce *linear probing* evaluation and some model analysis methods to reveal the secrets of pre-training, study the pattern of layer behaviors during pre-training and fine-tuning, and investigate what matters for downstream performances. For the sake of simplicity, we only investigate the ImageNet classification task and other downstream classification tasks shown in Tab. 3 and use the supervised pre-training baseline, the CL-based entries DINO [1] and MoCo-v3 [6], the best MIM-based entry MaskFeat [32], and the worst two MIM-based entries MAE [12] and SimMIM [28] in Tab. 3 for analysis in this section.

4.1 Linear Probing Evaluation

We first learn linear classifiers on frozen features for different classification tasks in our *linear probing* evaluation. It reflects how the representations obtained by the pre-trained models

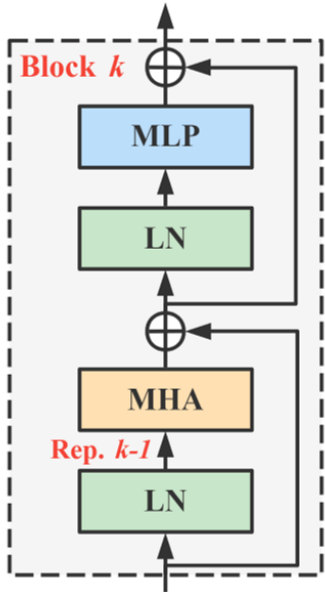


Fig. 2. **Transformer block**, where the feature map after the first LN of block k can be used as normalized output representation for block $k - 1$.

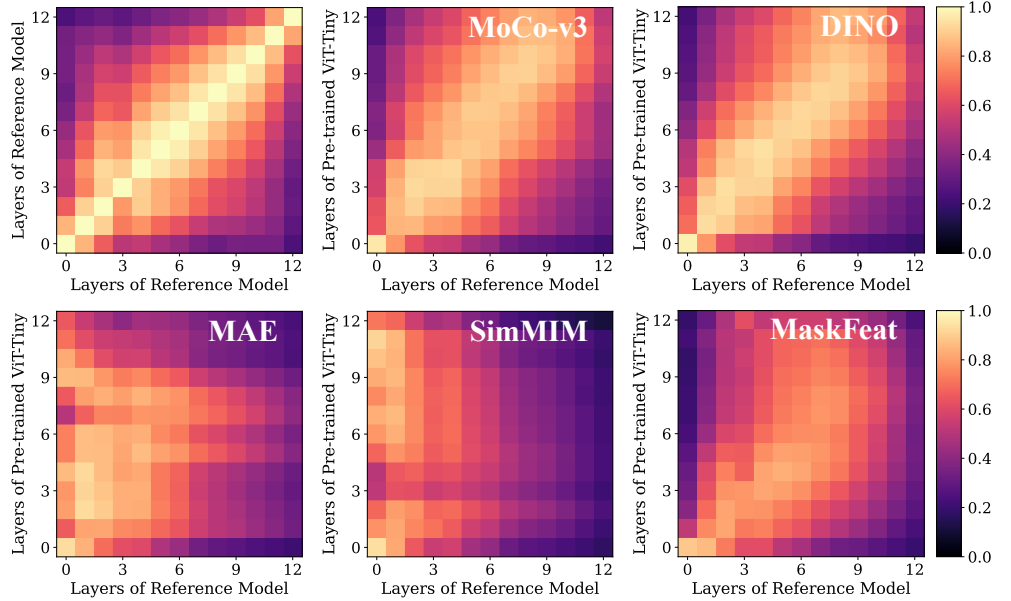


Fig. 3. **Layer representation similarity** as heatmaps for the investigated ViT-Tiny models from different pre-training methods, with x and y axes indexing the layers (the 0 index indicates the patch embedding layer), and higher values indicate higher similarity. The fully-supervised baseline based on our recipe (see Tab. 1) on IN1K is used as the reference.

TABLE 4
Linear Probing Evaluation of Pre-Trained Models on the Classification Tasks. Top-1 Accuracy Is Reported.

Methods	Datasets						
	Flowers	Pets	Aircraft	Cars	CIFAR100	iNat18	IN1K
<i>Supervised</i>							
Our Recipe	91.0	92.0	41.2	47.9	73.6	39.8	-
<i>CL</i>							
DINO	95.0	90.9	53.5	53.6	74.9	44.0	66.1
MoCo-v3	93.2	83.5	44.8	44.5	73.4	36.2	62.1
<i>MIM</i>							
MaskFeat	65.5	34.2	14.9	13.8	39.6	3.9	23.1
MAE	48.9	25.0	12.8	8.8	31.0	1.4	23.3
SimMIM	44.1	18.5	11.2	6.6	23.3	0.9	14.8

are linearly separable w.r.t. semantic categories. As shown in Tab. 4, the *linear probing* performance is consistently lower than the *fine-tuning* performance. Furthermore, while *linear probing* evaluation is informative for exploiting the pre-trained frozen models, it may not correspond to which models perform best after fine-tuned, especially for those downstream tasks with relatively sufficient labeled data, e.g., iNat18 and IN1K. In other words, it may lead to an underestimation of the value of some pre-trained models in the practical utility [12], [121] on downstream tasks. We attribute it to that *linear probing* only evaluates the final representation of the pre-trained models, which makes it overlook the value of providing good initialization for lower layers.

From another point of view, we think the failure of MIM-based self-supervised pre-training to perform better than CL-based models for the data-insufficient downstream tasks (as shown in Tab. 3) is due to the reason that CL pre-training learns more semantics at an abstract level relevant to recognition in higher layers than MIM pre-training, which also helps the frozen models from CL pre-training to achieve better *linear probing* evaluation results than MIM (as shown in Tab. 4). This analysis is already evident in the CL-based DINO [1] as its pre-training results show that the class-specific features can be automatically learned, even leading to unsupervised object

segmentation. This motivates us to further analyze the layer-wise representations and attention maps across and within different models to delve into the working mechanism of the different SSL pre-training methods for lightweight ViTs.

4.2 Layer-Wise Representation Analysis

We adopt the Centered Kernel Alignment (CKA) metric³ [138], [139] to analyze the layer-wise representation similarity across and within different models. Specifically, CKA takes two feature maps (or representations) X and Y as input and computes their normalized similarity $S(X, Y)$ in terms of the Hilbert-Schmidt Independence Criterion (HSIC [140]) as

$$S(X, Y) = \text{CKA}(K, L) = \frac{\text{HSIC}(K, L)}{\sqrt{\text{HSIC}(K, K)\text{HSIC}(L, L)}}, \quad (1)$$

where $K = XX^T$ and $L = YY^T$ denote the Gram matrices for the two feature maps, and the HSIC computation is invariant to the orthogonal transformation of representations and isotropic scaling. In our analyses, a mini-batch version of HSIC is adopted by using an unbiased estimator of HSIC [139] to work at scale compatible with our studied models. We select the normalized version of the output representation of each transformer block for computation, i.e., the feature map after the first LayerNorm (LN) [141] in its next block (see Fig. 2).

Analysis 1. We use heatmaps to visualize the layer-wise representation similarity of investigated pre-trained models with respect to a fully-supervised reference model in Fig. 3. We choose the fully-supervised baseline trained on the IN1K classification task based on our recipe (see Tab. 1) as the reference because we consider its representations are more recognition aligned and the higher similarity of the examined model’s layers to this supervised baseline can indicate more relevance to recognition for the examined model. Although the similarity does not directly indicate whether the downstream performance is good, it indeed reflects the pattern of layer representations to a certain extent. The similarity within the

3. <https://github.com/AntixK/PyTorch-Model-Compare>

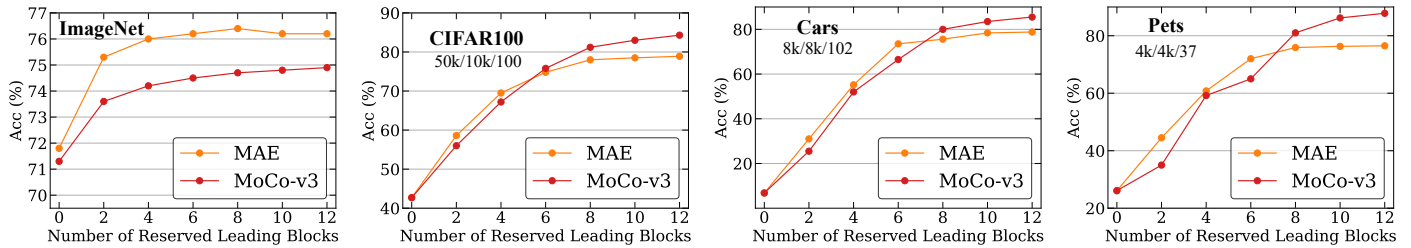


Fig. 4. Lower layers of the pre-trained ViT-Tiny models contribute to most gains on the data-sufficient IN1K. The contributions from higher layers of the pre-trained models increase as the downstream dataset scale shrinks, which indicates that higher layers matter in data-insufficient downstream tasks.

supervised baseline is also presented (see top-left of Fig. 3). In Sec. B.1, we also replace the above reference model with some much stronger ViT-Base reference models to test the robustness of our analysis.

We notice that lower layers matter more than higher ones if sufficient downstream data is provided. Specifically, we first observe a relatively high similarity between the models from MIM pre-training and the reference model for lower layers, while much lower similarity for higher layers. It indicates that fewer semantics are extracted from MIM pre-training at a more abstract level in higher layers. In contrast, the models from CL pre-training aligns the reference model well across almost all layers. However, the fine-tuning evaluation on IN1K (see Tab. 1) shows that adopting MIM pre-training as the initialization improves the performance more significantly than CL pre-training. Thus, we hypothesize that *lower layers matter much more than higher ones for the self-supervised pre-training methods to perform well on the data-sufficient IN1K*. In order to verify the hypothesis, we design another experiment by sweeping over the number of reserved consecutive leading blocks of pre-trained models for initialization (the remaining blocks after the reserved blocks are randomly initialized), and then fine-tuning the initialized models on IN1K (for the sake of simplicity, we adopt 100-epoch fine-tuning). The left figure of Fig. 4 shows that reserving only a certain number of leading blocks at the lower end can already achieve a significant performance gain over randomly initializing all the blocks (*i.e.*, totally training from scratch) for both MIM-based MAE and CL-based MoCo-v3 pre-training. Whereas, further reserving higher layers leads to marginal gains for both of them, which demonstrates our hypothesis.

Analysis 2. We further conduct similar experiments to the above setting on some small-scale downstream datasets, and find that *higher layers matter in data-insufficient downstream tasks*. The results are shown in the remaining figures of Fig. 4. We observe consistent performance improvements as the number of reserved pre-trained models’ leading blocks increases. And the smaller the dataset scale, the more the performance benefits from the higher layers. It demonstrates that higher layers are still valuable and matter in data-insufficient downstream tasks. Furthermore, we observe comparable performance for the transfer evaluation of both MAE and MoCo-v3 pre-training when only a certain number of lower layers are reserved for initialization, while CL-based MoCo-v3 surpasses MIM-based MAE when higher layers are further reserved. It indicates that the higher layers of MoCo-v3 pre-trained models work better than MAE on data-insufficient downstream tasks, which is also consistent with our CKA-based analysis shown in Fig. 3, that CL pre-training learns more semantics at an abstract level relevant to recognition in higher layers (high similarity to the recognition-aligned reference model in higher layers).

4.3 Attention Map Analysis

The attention maps can reveal the behaviors for aggregating information in the attention mechanism of ViTs, which are computed from the compatibility of queries and keys by dot-product operation. We introduce two metrics for further analysis based on the attention maps: (1) the attention distance, which is defined as (for the j_{th} token of the h_{th} head)

$$D_{h,j} = \sum_{i=1}^l \text{softmax}(\mathbf{A}_h)_{i,j} G_{i,j}, \quad (2)$$

where $\mathbf{A}_h \in \mathbb{R}^{l \times l}$ is the attention map for the h_{th} attention head, $G_{i,j}$ is the Euclidean distance between the spatial locations of the i_{th} and j_{th} tokens, and l is the number of tokens; (2) the attention entropy, which is defined as

$$E_{h,j} = - \sum_{i=1}^l \text{softmax}(\mathbf{A}_h)_{i,j} \log(\text{softmax}(\mathbf{A}_h)_{i,j}). \quad (3)$$

Then, the average attention distance and attention entropy across all tokens in the h_{th} head can be calculated as

$$d_h = \frac{1}{l} \sum_{j=1}^l D_{h,j} \quad \text{and} \quad e_h = \frac{1}{l} \sum_{j=1}^l E_{h,j}. \quad (4)$$

Specifically, the average attention distance for one head reveals how much local *vs.* global information is aggregated, and a lower distance indicates that on average each token focuses more on neighbor tokens in this head. The average attention entropy for one head reveals the concentration of the attention distribution, and a lower entropy indicates that on average each token attends to fewer tokens. We use the models pre-trained with MoCo-v3, DINO, MAE, SimMIM and MaskFeat respectively for the attention map analysis in Fig. 5 and conduct the layer-by-layer analysis for the distributions of the average attention distance and entropy across all the different attention heads of the examined models.

Analysis 3. We first focus on the comparison between the MIM pre-trained and CL pre-trained models, trying to give some explanations for their diverse downstream performances observed in Sec. 3. As shown in the left column of Fig. 5, we observe that MoCo-v3 pre-training generally results in more global and broad attention than MAE. Even several leading blocks have a narrower range of attention distance and entropy than MAE. Compared with the randomly initialized model, *the MAE pre-trained model has significantly lower attention distance and entropy, which means that MAE pre-training noticeably introduces locality inductive bias*. This is consistent with the practice in [14] that the authors opt to teach the locality bias to the simple hierarchical ViT model Hiera using MAE pre-training while avoiding adding it through vision-specific modules like shifted windows or convolutions. As for the

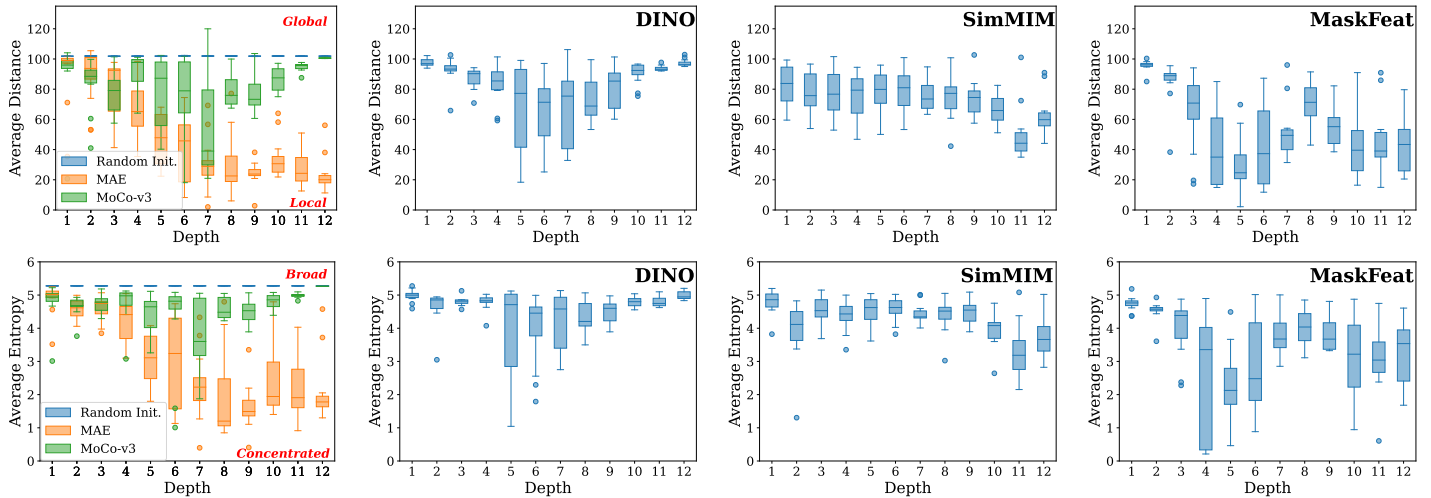


Fig. 5. **Attention distance and entropy analyses.** We visualize the layer-by-layer distributions of the average attention distance and entropy across all the different attention heads using the box-whisker plots. We specifically plot the MAE pre-trained and MoCo-v3 pre-trained ViT-Tiny models along with the randomly initialized one in the same figures (see left) for a more intuitive and compact comparison.

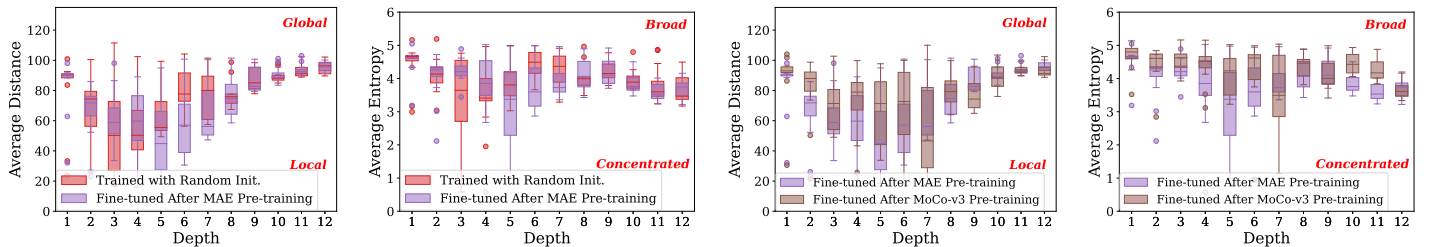


Fig. 6. **Attention distance and entropy analyses for the ViT-Tiny models fine-tuned on IN1K.** We compare the fine-tuned model after MAE pre-training with the fully-supervised one with random initialization in the left, while the comparison with MoCo-v3 is in the right.

other pre-trained models in Fig. 5, we can see that SimMIM also tends to make the model focus on local patterns with concentrated attention in higher layers like MAE, while DINO pre-training behaves like MoCo-v3 and results in broad and global attention in higher layers. It is noteworthy that the locality inductive bias does not mean that tokens in all attention heads attend to solely a few nearby tokens. The attention distance and entropy for different heads are still distributed in a wide range (except several last layers), which indicates that the heads have diverse specializations, making the models aggregate both local and global tokens with both concentrated and broad focuses.

We then analyze how the entries in the left column of Fig. 5 behave when fine-tuned or trained on the downstream IN1K classification task. As shown in Fig. 6, we find that *the pre-training with MAE makes the attention of its downstream fine-tuned model more local and concentrated than others.* First, we compare the fine-tuned model based on MAE pre-training with the fully-supervised one (random initialization) in the left of Fig. 6. We observe very similar attention behaviors between them, except that the attention with MAE pre-training is more local (with lower attention distance) and concentrated (with lower attention entropy) in middle layers compared with the fully-supervised one. Second, we conduct the attention comparison for the fine-tuned models with MAE and MoCo-v3 pre-training in the right of Fig. 6. It is shown that the fine-tuned model with MoCo-v3 pre-training still has more broad and global attention than the one with MAE pre-training in the middle layers.

As the MoCo-v3 pre-trained model generally has more global and broad attention than the MAE pre-trained one, we think this characteristic of MoCo-v3 makes its downstream fine-tuning take “shortcuts”, *i.e.*, directly paying attention to global features and overlooking local patterns, which may

be unfavorable for more fine-grained recognition when the downstream data for fine-tuning is sufficient. It leads to inferior downstream performance on IN1K. As for the MAE pre-trained model, its distinct behaviors in higher layers with rather low attention distance and entropy may make it hard to be successfully transferred to data-insufficient downstream tasks, thus resulting in inferior performance on these tasks.

5 SOLUTION

In the previous section, we have conjectured that it is hard for MIM pre-training, especially the MAE-based, to learn good representations relevant to recognition in higher layers, which results in unsatisfactory performance on data-insufficient downstream tasks, though providing good initialization only for lower layers contributes to notable performance improvement on downstream tasks with large-scale training data. A natural question that arises is can the MIM pre-training gain more high-level semantic information by scaling up the models. We further examine a large ViT-Base model with MAE pre-training [12] in Fig. 7, and find it achieves a better alignment with our used reference model based on ViT-Tiny (the fully-supervised baseline based on our recipe in Fig. 3). It indicates that *it is possible to extract features relevant to recognition in higher layers for the up-scaled encoder in MAE pre-training, and the pre-trained large model has more global and broad attention in higher layers.* This observation motivates us to compress the knowledge of large pre-trained models to lightweight ones with knowledge distillation under the MIM framework (without relying on the training set labels), *e.g.*, applying knowledge distillation during the MAE pre-training phase for lightweight ViTs.

It is a common practice to utilize soft target probabilities (soft labels), features and intermediate representations to per-

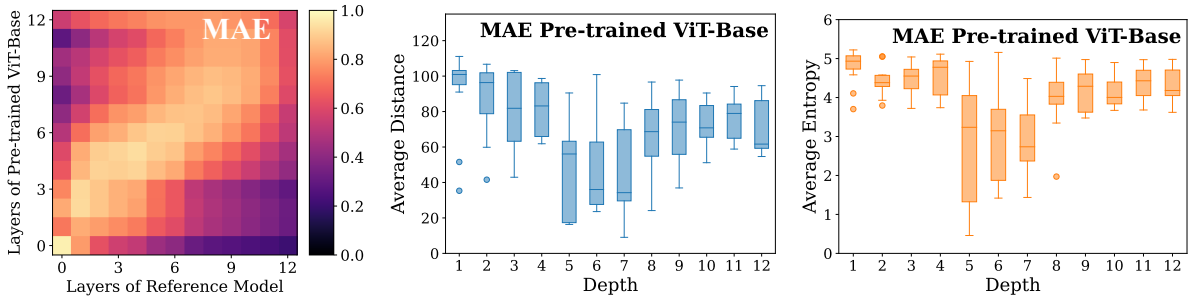


Fig. 7. The ViT-Base model with MAE pre-training [12] can achieve a better alignment with our used reference model in Fig. 3. Its higher layers exhibit more global and broad attention than its lightweight ViT-Tiny counterpart with MAE pre-training.

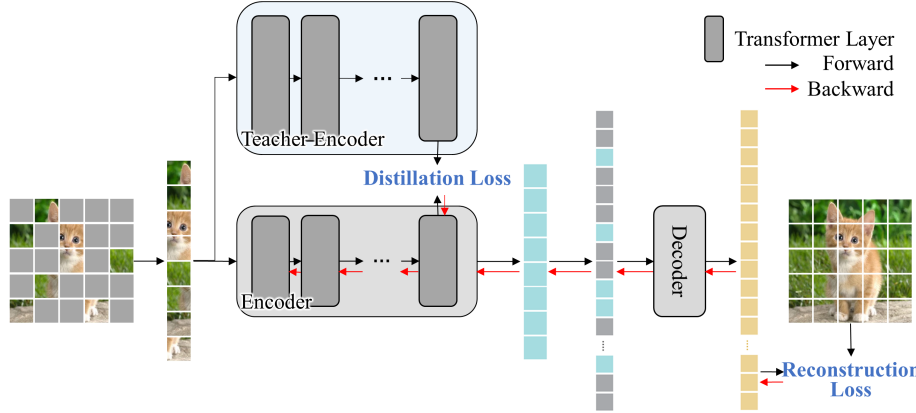


Fig. 8. Illustration of our MAE pre-training with distillation on lightweight ViTs. The teacher (MAE pre-trained ViT-Base) processes the same visible image patches as the student encoder.

form knowledge distillation. For instance, some works [106], [107], [108], [109] perform distillation to obtain pre-trained compressed language models by exploiting soft target probabilities for masked language modeling predictions, embedding layer outputs, self-attention distributions or output representations (hidden states for the transformer blocks) from the teacher models to guide the student pre-training. As there are many distillation target alternatives and distillation strategies that could be explored, we only consider the most intuitive factors investigated in Sec. 4 for distillation in our work, which are the layer-wise representations and attention maps. Our aim is to obtain good representations for the higher layers of lightweight ViTs to make them have high similarity to the recognition-aligned reference model (or the large pre-trained teacher model). We can thus distill the layer-wise representations explicitly or obtain the good representations implicitly through distilling the attention maps.

5.1 Improve MAE Pre-Training Based on Distillation

We herein introduce our distillation process in the MAE pre-training framework (as illustrated in Fig. 8) to showcase the effectiveness of our observation-analysis-solution flow in improving the MIM pre-training of ViT-Tiny on higher layers. Based on the masked autoencoder framework, we introduce our examined MAE pre-trained ViT-Base model in Fig. 7 as the teacher. During the MAE pre-training of ViT-Tiny, the teacher processes the same visible image patches as the student encoder ViT-Tiny, and two kinds of layer-wise attention-based and representation-based distillation losses can be constructed between the corresponding teacher’s and student’s layers for our investigation. The parameters of the student are updated based on the joint backward gradients from the distillation loss and the original MAE’s reconstruction loss, while the teacher’s parameters remain frozen throughout the pre-training process.

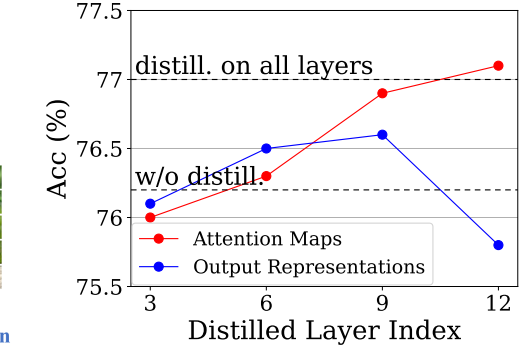


Fig. 9. Distillation on attention maps of higher layers significantly improves the performance over the pre-training baseline without distillation.

The original MAE’s reconstruction loss is constructed by using the output of the last layer of the student encoder as the decoder’s input.

We construct the layer-wise attention-based and representation-based distillation losses as follows respectively based on the mean squared error (MSE):

$$L_{\text{attn}} = \text{MSE}(\mathbf{A}_t, \mathbf{M}\mathbf{A}_s), \quad (5)$$

$$L_{\text{rep}} = \text{MSE}(\mathbf{X}_t, \mathbf{X}_s\mathbf{N}), \quad (6)$$

where $\mathbf{A}_t \in \mathbb{R}^{h \times l \times l}$ and $\mathbf{A}_s \in \mathbb{R}^{h' \times l \times l}$ refer to the attention maps of the corresponding teacher’s and student’s layers, with h and h' attention heads respectively. l is the number of tokens. A learnable mapping matrix $\mathbf{M} \in \mathbb{R}^{h \times h'}$ is introduced to align the number of heads. $\mathbf{X}_t \in \mathbb{R}^{l \times d}$ and $\mathbf{X}_s \in \mathbb{R}^{l \times d'}$ are the output representations of the corresponding teacher’s and student’s layers, with hidden dimensions as d and d' respectively. $\mathbf{N} \in \mathbb{R}^{d' \times d}$ is also a learnable mapping matrix.

Distill on attention maps or output representations? We conduct a fine-tuning performance comparison (100 epochs for the sake of simplicity) on IN1K for the utilization of the two kinds of different distillation targets during our MAE pre-training (400 epochs). We test the distillation on the 3rd, 6th, 9th and 12th layers individually, *i.e.*, the distillation losses are constructed between the pairs of layers at 1/4, 2/4, 3/4 and 4/4 depth of the teacher and student respectively. As shown in Fig. 9, distillation on the attention maps of the last transformer blocks promotes the performance most, not only surpassing the same kind of distillation on lower layers, but also contributing to more performance gain in comparison to the distillation on the output representations. It is consistent with the analyses in Sec. 4. On the one hand, the lower layers learn good representations themselves during the MAE pre-training without distillation, and thus distillation on these layers contributes to marginal improvements, though

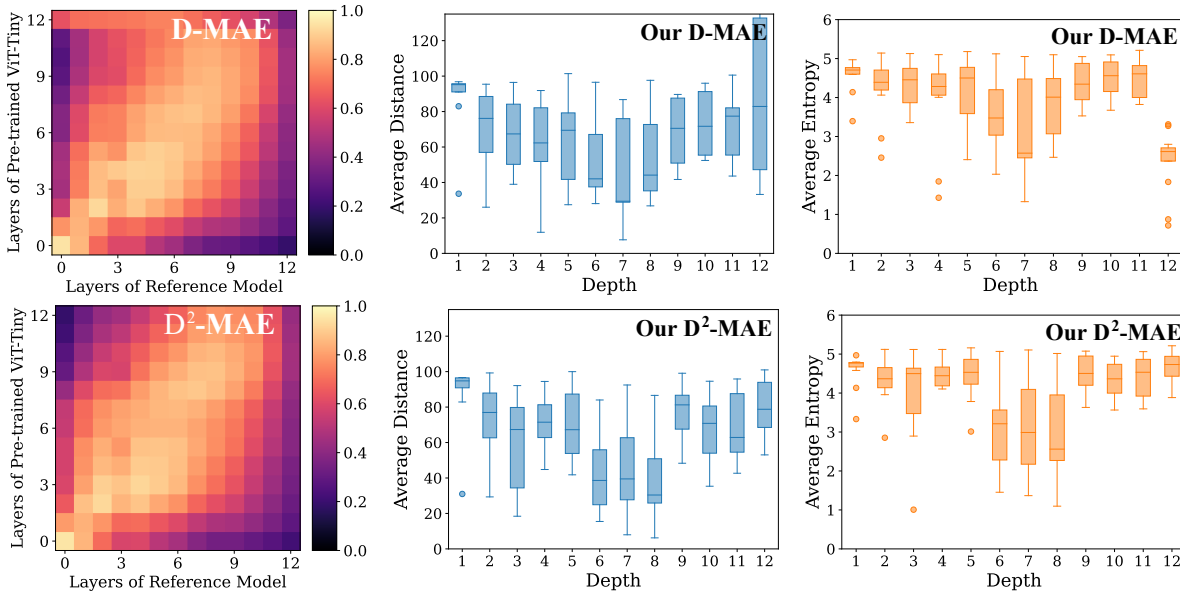


Fig. 10. Distillation compresses the good representation of the ViT-Base teacher to the student through our D-MAE or D²-MAE pre-training. The distilled student shows higher layer-wise representation similarity to our used fully-supervised reference model in Fig. 3. Our D²-MAE pre-training further improves the behavior patterns of the attention weights on higher layers, especially on the 12th layer.

TABLE 5
Sweep Over the Intermediate Layer Index to Which the Decoder for Reconstruction Is Connected. Top-1 Accuracy for Classification Tasks and AP for Detection Tasks Are Reported.

Datasets	Encoder Layer Index for Reconstruction						
	w/o [◇]	2	4	6	8	10	12
COCO (det.)	39.6	41.8	42.2	42.2	42.3	42.1	42.0
Pets	84.5	87.6	89.5	89.9	90.4	91.2	89.1
Cars	80.3	86.0	87.6	88.4	88.2	87.9	87.5
CIFAR100	82.1	84.8	85.2	85.3	85.2	85.2	85.0

[◇] indicates using distillation for pre-training without reconstruction.

distillation on the output representations directly performs a little better than on the attention maps of these layers. On the other hand, the higher layers rely on a good teacher to guide them to capture rich semantic features, and the attention weights on the higher layers of the teacher exhibit some patterns of behavior with much richer semantic knowledge, which may be the reason for the attention map’s superiority over the representation for distillation on higher layers. Fig. 7 also shows that the representations deteriorate on the 12th layer for the MAE pre-trained ViT-Base.

We denote the above best MAE pre-training based on attention map distillation on the last layer as D-MAE. As show in the top-left subfigure of Fig. 10, the CKA analysis for the D-MAE pre-trained ViT-Tiny indicates that the rich semantic knowledge of the teacher has been successfully transferred to the pre-trained lightweight student.

5.2 Decoupled Distillation Further Improves Pre-Training

Despite the successfully obtained good representation with D-MAE, it is shown in Fig. 10 that the attention weights on the 12th layer of the obtained ViT-Tiny exhibit some weird behavior patterns, *i.e.*, the distributions of the average attention distance and entropy cover a wide range of values while the entropy values are significantly lower than on other higher layers. That is to say the tokens in some heads of this last layer only attend to very few far away tokens while some focus on very few neighbor tokens. We think a reason for this is

due to the conflict between distillation of high-level semantic knowledge and reconstruction of low-level pixels during MAE pre-training when these two tasks are both applied to the last layer, leading to a bad compromise for the different heads to learn the attention. To avoid this conflict, we propose a decoupled distillation strategy in this section.

Decoupled distillation strategy. As shown in Fig. 3, the deterioration of representation learning on higher layers in the original MAE pre-training of lightweight ViTs indicates that there is some homogeneity among the representation learning of higher layers during the MAE reconstruction of the RGB pixel targets. That means it is not necessary to rely on the last layer for reconstructing the targets. We thus decouple the distillation task from the MAE reconstruction task by connecting the decoder for reconstruction to other intermediate layers of the student ViT-Tiny instead of the last layer during pre-training in Fig. 8. We conduct a sweep over the intermediate layer index ranging from 2 to 12 for the optimal decoupled distillation. The fine-tuning results on some selected datasets (see Tab. 5) show that connecting to the 6th, 8th, or 10th layer can all further improve the performance over the model based on D-MAE (*i.e.*, the column with the encoder layer index of 12 for reconstruction in Tab. 5). We use the 8th encoder layer for MAE reconstruction in the subsequent experimental analysis and validation by default, and denote this pre-training with decoupled distillation as D²-MAE. It can be seen in Fig. 10 that the attention weights on the higher layers after D²-MAE pre-training exhibit very similar behavior patterns to the ViT-Base teacher (see Fig. 7).

In Tab. 5, we also test the scenario of only relying on the attention map distillation to achieve good representation for the lightweight ViT model, *i.e.*, the MAE reconstruction loss in Fig. 8 is abandoned. It is shown that the experimental results without reconstruction are significantly lower than using both the distillation and reconstruction. However, only relying on the attention map distillation has already slightly surpassed the MAE pre-training without distillation for ViT-Tiny. This further demonstrate the effectiveness and superiority of our observation-analysis-solution flow for developing the attention map distillation-based solution.

TABLE 6

Distillation Significantly Improves Performance on Various Tasks. Top-1 Accuracy Is Reported for Classification Tasks, mIoU Is for ADE20K Segmentation, AUC Is for LaSOT Tracking, and AP Is for COCO Detection (Det.) and Segmentation (Seg.).

Methods	Datasets		Classification Tasks					Dense Prediction Tasks		
	Flowers	Pets	Aircraft	Cars	CIFAR100	iNat18	IN1K	ADE20K	LaSOT	COCO (det./seg.)
<i>Supervised (IN1K)</i>										
Our Recipe	96.4	93.1	73.5	85.6	85.8	64.7	76.5	41.5	64.1	40.4/35.5
<i>MAE Self-Supervised</i>										
MAE	85.8	76.5	64.6	78.8	78.9	64.0	78.0	34.5	61.6	39.9/35.4
D-MAE	95.2	89.1	79.2	87.5	85.0	65.7	78.3	42.9	65.8	42.3/37.3
D ² -MAE	96.0	90.4	80.0	88.2	85.2	66.2	78.7	43.3	66.1	42.5/37.5
Δ to MAE	+10.2	+13.9	+15.4	+9.4	+6.3	+2.2	+0.7	+8.8	+4.5	+2.6/+2.1
Δ to Supervised Pre-train	-0.4	-2.7	+6.5	+2.6	-0.6	+1.5	+2.2	+1.8	+2.0	+2.1/+2.0

5.3 Performance Improvements Based on Distillation

We finally evaluate our distillation-based MAE pre-trained models on all the classification and dense prediction tasks exploited in the observation section (Sec. 3). As shown in Tab. 6, our distillation contributes to significant performance improvements over the MAE pre-training without distillation, especially on the data-insufficient classification tasks and dense prediction tasks. In comparison to the supervised pre-training baseline (Our Recipe) relying on IN1K labels, our distillation-based MAE pre-training not only saves the costs for labeling the pre-training data, but also provides richer learning signals and avoids the bias towards the pre-defined set of IN1K labels. This leads to performance gains on Aircraft, Cars, iNat18, *etc.*, which may contain less overlapped categories or domains with ImageNet than Flowers, Pets and CIFAR100. The decoupled distillation strategy D²-MAE also consistently improves over D-MAE on all the evaluated datasets.

6 STATE-OF-THE-ART COMPARISON RESULTS

In this section, we mainly compare the obtained models, which are based on optimized pre-training strategies following our observation-analysis-solution flow, to the recent SOTA methods in the lightweight regime. We conduct the comparison on the ImageNet classification task, COCO object detection and instance segmentation tasks, ADE20K semantic segmentation task, and LaSOT single object tracking task.

As we have stated in Observation 2 of Sec. 3, our studying of MAE pre-training on lightweight ViTs is orthogonal to the network architecture design methodology in the ViT derivatives. We thus also apply our approach on the hierarchical vision transformer Hiera [14] to demonstrate the superiority of our observation-analysis-solution flow. Hiera [14] is an extremely simple framework that is more accurate than previous models (*e.g.*, the MViT family [142], [143]) while being significantly faster both at inference and during training. Hiera avoids some redundant constraints used in MViTv2 [143], *i.e.*, the convolutional structure and decoupled relative position encoding. It also incorporates the local attention (*i.e.*, mask unit attention) in the first two stages of the model and keeps the capability to perform sparse MAE pre-training (*i.e.*, masked tokens are deleted). We resize the smallest model of Hiera in the original paper to a lightweight size to obtain the Hiera-Tiny with only a 6.5M parameter count. Specifically, we only modify the initial embedding dimension to 46 to make it match the lightweight vanilla ViT model ViT-Tiny used in our paper, leaving other components including the number of heads, blocks, *etc.* unchanged.

Our observation and analysis on Hiera-Tiny are almost the same as that on ViT-Tiny, so we can directly apply our decoupled distillation on its MAE pre-training to improve the performance. It is noteworthy that we evaluate performance for Hiera-Tiny in this section only on the ImageNet classification task and COCO object detection and instance segmentation tasks following the original paper to achieve the image results due to its intrinsic hierarchical property. In Sec. C.1, we also show that our distillation technique D-MAE can help other-scale vanilla ViT students beyond ViT-Tiny to achieve better downstream performance.

6.1 Comparison on ImageNet Classification

In Tab. 7, we compare both the enhanced ViT-Tiny and Hiera-Tiny with our distillation-based MAE pre-training to the current lightweight ConvNets and ViT derivatives. We report top-1 accuracy along with the model parameter count and the latency. By taking inspiration from the commonly used strategies in the network architecture design methodology, such as extending the supervised fine-tuning duration to a much longer schedule and using relative position bias, our approach can further benefit from them to achieve 79.4%/78.9% top-1 accuracy on ImageNet-1K, which is comparable to the current SOTA networks with sophisticated architecture design. It means that our proposed distillation strategy for the MAE pre-training can unleash the great potential of the *extremely simple* lightweight ViTs, which is commonly overlooked in the past several years. Although some of the hierarchical ViTs (*e.g.*, LeViT-192, EfficientFormerV2-S1 and EfficientViT-B1) enjoy higher accuracy and more attractive latency than ours simultaneously, our pre-training enables the more versatile ViT model ViT-Tiny to be outstanding on both the ADE20K semantic segmentation and LaSOT single object tracking tasks in the lightweight regime (see Sec. 6.3 and Sec. 6.4 below).

6.2 Comparison on COCO Detection and Segmentation

For a more thorough study, we further conduct the SOTA comparison on the downstream object detection and segmentation tasks of COCO [132]. As we have detailed in Sec. 3.3, we reproduce and rigorously follow the benchmarking setup in the Mask R-CNN framework in [135] except for some minimal changes to the training settings. In specific, the different models in Tab. 8 are used for the initialization of the backbone. Our pre-training not only improves over the supervised pre-training significantly, but also makes the *extremely simple* hierarchical Hiera-Tiny

TABLE 7

Comparison Results to the Current SOTA Lightweight Models on ImageNet-1K. Top-1 Accuracy on Its Validation Set with Parameter Count and Latency Are Reported. All Models Are Tested on Input Scale of 224×224 , Except That MobileViT [21] and FastViT [24] Are Tested with 256×256 According to Their Original Papers. ‘bsn’ Means the Latency Is Measured with Batch Size n .

Models	Publication	Pre-Training		Fine-Tuning		Params↓	Latency↓		Top-1 Acc.↑ (%)
		Methods	Data	Distill.	#Epochs		Orin (bs1)	A100 (bs16)	
<i>ConvNets Family</i>									
ResNet-18 [74]	CVPR’16	-	-	✗	100	11.7M	0.99ms	1.12ms	69.7
EfficientNet-B0 [81]	ICML’19	-	-	✗	450	5.3M	2.36ms	2.30ms	77.7
EfficientNet-B1 [81]	ICML’19	-	-	✗	450	7.8M	3.15ms	3.00ms	78.8
MobileNet-v3 [82]	ICCV’19	-	-	✗	600	5.5M	1.55ms	1.63ms	75.2
MobileNet-v3 [†] [144]	CVPR’22	Supervised	IN21K	✓	600	5.5M	1.55ms	1.63ms	77.9
ConvNeXt V1-F [80]	CVPR’22	-	-	✗	600	5.2M	3.06ms	3.13ms	77.5
ConvNeXt V2-F [†] [66]	CVPR’23	FCMAE [66]	IN1K	✗	600	5.2M	4.35ms	4.09ms	78.5
<i>Non-Hierarchical ViTs</i>									
XCiT-T12/16 [18]	NeurIPS’21	-	-	✓	400	6.7M	7.20ms	6.03ms	78.6
CaiT-XXS-24 [20]	ICCV’21	-	-	✓	400	12.0M	8.96ms	7.25ms	78.4
DeiT-Tiny [16]	ICML’21	-	-	✗	300	5.7M	3.35ms	2.48ms	72.2
DeiT-Tiny [†] [16]	ICML’21	-	-	✓	1000	5.7M	3.35ms	2.48ms	76.6
<i>Hierarchical ViTs</i>									
LeViT-128 [17]	ICCV’21	-	-	✓	1000	9.2M	2.61ms	2.28ms	78.6
LeViT-192 [17]	ICCV’21	-	-	✓	1000	11.0M	2.83ms	2.36ms	80.0
PiT-Ti [19]	ICCV’21	-	-	✓	1000	5.1M	3.80ms	2.85ms	76.4
Swin-1G [22], [86]	CVPR’22	-	-	✗	450	7.3M	3.28ms	3.17ms	77.3
MobileFormer-294M [22]	CVPR’22	-	-	✗	450	11.4M	9.71ms	6.86ms	77.9
EdgeViT-XS [23]	ECCV’22	-	-	✗	300	6.7M	4.95ms	4.12ms	77.5
MobileViT-S [21]	ICLR’22	-	-	✗	300	5.6M	3.93ms	3.72ms	78.3
FastViT-T12 [24]	ICCV’23	-	-	✗	300	6.8M	2.85ms	3.13ms	79.1
EfficientFormerV2-S1 [25]	ICCV’23	-	-	✓	450	6.1M	3.37ms	3.04ms	79.7
EfficientViT-M4 [145]	CVPR’23	-	-	✓	1000	8.8M	4.06ms	2.90ms	77.1
SeaFormer-L [27]	ICLR’23	-	-	✗	600	14.0M	5.12ms	4.01ms	79.9
EfficientViT-B1 [26]	ICCV’23	-	-	✗	300	9.1M	2.42ms	2.40ms	79.4
<i>Ours</i>									
ViT-Tiny	-	-	-	✗	300	5.7M	4.01ms	3.20ms	75.8
	MAE [12]	IN1K	-	✗	300	5.7M	4.01ms	3.20ms	78.0
	D ² -MAE	IN1K	-	✗	300	5.7M	4.01ms	3.20ms	78.7
	D ² -MAE [‡]	IN1K	-	✗	1000	5.7M	4.01ms	3.20ms	79.4
Hiera-Tiny	-	-	-	✗	300	6.5M	3.08ms	3.12ms	75.8
	MAE [14]	IN1K	-	✗	300	6.5M	3.08ms	3.12ms	78.5
	D ² -MAE	IN1K	-	✗	300	6.5M	3.08ms	3.12ms	78.9

[†] indicates that the corresponding models are further improved based on an additional pre-training stage for model initialization.

[‡] indicates that our initialized ViT-Tiny additionally adopt the relative position embedding (RPE) trick used in [28] during fine-tuning. Note that Hiera-Tiny can benefit from neither this RPE trick nor the longer fine-tuning schedule.

TABLE 8

Comparison Results to Previous SOTA Lightweight Models in the Mask R-CNN Framework on COCO.

Backbones	#Param.	FLOPs	Pre-Train	AP ^{bb}	AP ^{bb} ₅₀	AP ^{bb} ₇₅	AP ^m	AP ^m ₅₀	AP ^m ₇₅
ResNet18 [74]	31M	207G	Super.	37.1	57.3	40.0	34.0	54.3	36.4
ResNet50 [74]	44M	260G	Super.	41.0	61.7	44.9	37.1	58.4	40.1
PVT-T [88]	33M	208G	Super.	39.8	62.2	43.0	37.4	59.3	39.9
LightViT-T [146]	28M	187G	Super.	41.5	64.4	45.1	38.4	61.2	40.8
ViT-Tiny	28M	204G	Super.	40.4	60.7	43.1	35.5	56.8	36.9
			D ² -MAE	42.5	62.6	45.6	37.5	59.4	39.4
Hiera-Tiny	28M	205G	Super.	37.9	58.7	40.4	34.3	55.5	35.9
			D ² -MAE	43.2	64.0	46.7	38.7	60.7	41.4

TABLE 9
Comparison Results to Lightweight Semantic Segmentation Methods on ADE20K.

Backbones	#Param.	FLOPs	Pre-Train	mIoU
<i>High-resolution Segmentation-specific</i>				
SeaFormer-L [27]	14.0M	6.5G	Super.	42.7
EfficientViT-B1 [26]	4.8M	6.3G	Super.	42.8
<i>Versatile Backbones with Semantic-FPN Decoder</i>				
ResNet18 [74]	15.4M	32.3G	Super.	34.1
LeViT-192 [17]	14.7M	10.2G	Super.	34.8
PVT-T [88]	17M	16.6G	Super.	35.7
LightViT-T [146]	12.2M	33.1G	Super.	39.9
ViT-Tiny	7.0M	13.5G	Super.	38.0
			D ² -MAE	39.0
			Super.*	41.5
			D ² -MAE*	42.8

* indicates the models adopt an intermediate 1000-epoch fine-tuning on IN1K classification before ADE20K segmentation fine-tuning.

to outperform the delicately designed convolution-free ViT derivatives PVT-T and LightViT-T.

6.3 Comparison on ADE20K Semantic Segmentation

We also conduct the SOTA comparison on the downstream semantic segmentation task of ADE20K [133]. To align with the recent effort on reducing the computational cost of high-resolution dense prediction to ease its deploying on hardware devices, *e.g.*, the segmentation-specific models SeaFormer and EfficientViT, we instead use the Semantic-FPN framework [153] to evaluate the different lightweight versatile backbones in Tab. 9. It can be seen that the image classification-proficient model LeViT with decreasing resolutions can not perform well on this ADE20K dense prediction task, while our pre-training with intermediate fine-tuning on IN1K enables ViT-Tiny to achieve comparable accuracy with the segmentation-specific models.

6.4 Comparison on LaSOT Visual Tracking

We finally conduct the SOTA comparison on the downstream single object visual tracking task of LaSOT [133] in the lightweight regime, in which the real-time running on limited computing resources such as CPU is required. As we have detailed in Sec. 3.3, we reproduce and rigorously follow the original setup in the speed-oriented version of the SOTA tracker OTrack [137] (256×256 input size of search patch) except that we only replace the backbone for joint feature extraction and relation modeling with different pre-trained ViT-Tiny, namely OTrack-T in Tab. 10. It shows that our pre-training enhances OTrack-T to outperform all the current SOTA lightweight CPU-realtime trackers and set a new record of 66.1% AUC on LaSOT.

7 CONCLUSION

In this paper, we investigate an easily overlooked aspect of obtaining strong lightweight ViTs through MIM pre-training, which is optimizing the pre-training strategies for improving the *extremely simple* lightweight ViTs and hence orthogonal to the delicate design of ViT derivatives by

TABLE 10
Comparison Results to Previous SOTA Lightweight CPU-Realtime Trackers on LaSOT. We Report CPU Runtime Speeds in FPS.

Trackers	Backbones	#Param.	FLOPs	Pre-Train	AUC	Speed
HiT-Base [147]	LeViT-384	42.1M	4.3G	Super.	64.6	33
HiT-Small [147]	LeViT-128	11.0M	1.1G	Super.	60.5	72
HiT-Tiny [147]	LeViT-128S	9.6M	1.0G	Super.	54.8	76
LightTrack-L [148]	LT-Mobile	3.1M	0.8G	Super.	55.5	-
LightTrack-M [148]	LT-Mobile	2.0M	0.5G	Super.	53.8	41
E.T.Track [149]	LT-Mobile	7.0M	1.7G	Super.	59.1	47
FEAR-L [150]	RegNet	4.1M	4.9G	Super.	57.9	-
FEAR-XS [150]	FBNet	1.0M	1.0G	Super.	53.5	60
HCAIT [151]	ResNet18	6.8M	1.3G	Super.	59.3	45
MixFormerV2-S [152]	ViT-Base	16.2M	4.4G	Super.	60.6	30
OTrack-T	ViT-Tiny	8.0M	1.9G	Super.	64.1	41
				D-MAE	65.8	41
				D ² -MAE	66.1	41

introducing sophisticated components with inductive biases. Our comprehensive analyses and investigations reveal several key factors that hide behind the achieved superior results, the value of which has also been demonstrated as it guides the design of our proposed distillation strategy for better MIM pre-training. We believe the observations, analyses and solutions in this paper will improve the understandings of MIM pre-training for lightweight ViTs, and we expect our observation-analysis-solution flow will further advance the SSL-based pre-training research.

REFERENCES

- [1] M. Caron, H. Touvron, I. Misra, H. Jégou, J. Mairal, P. Bojanowski, and A. Joulin, "Emerging properties in self-supervised vision transformers," in *Proc. Int. Conf. Comput. Vis.*, 2021, pp. 9650–9660.
- [2] K. He, H. Fan, Y. Wu, S. Xie, and R. Girshick, "Momentum contrast for unsupervised visual representation learning," in *Proc. IEEE Conf. Comput. Vis. Pattern Recognit.*, 2020, pp. 9729–9738.
- [3] X. Chen, H. Fan, R. Girshick, and K. He, "Improved baselines with momentum contrastive learning," *ArXiv*, vol. abs/2003.04297, 2020.
- [4] J.-B. Grill, F. Strub, F. Altché, C. Tallec, P. Richemond, E. Buchatskaya, C. Doersch, B. Pires, Z. Guo, M. Azar *et al.*, "Bootstrap your own latent: A new approach to self-supervised learning," in *Proc. 34th Conf. Adv. Neural Info. Process. Syst.*, 2020.
- [5] M. Caron, I. Misra, J. Mairal, P. Goyal, P. Bojanowski, and A. Joulin, "Unsupervised learning of visual features by contrasting cluster assignments," in *Proc. Int. Conf. Adv. Neural Info. Process. Syst.*, 2020.
- [6] X. Chen, S. Xie, and K. He, "An empirical study of training self-supervised vision transformers," in *Proc. Int. Conf. Comput. Vis.*, 2021, pp. 9640–9649.
- [7] J. Deng, W. Dong, R. Socher, L.-J. Li, K. Li, and L. Fei-Fei, "ImageNet: A large-scale hierarchical image database," in *Proc. IEEE Conf. Comput. Vis. Pattern Recognit.*, 2009, pp. 248–255.
- [8] Z. Fang, J. Wang, L. Wang, L. Zhang, Y. Yang, and Z. Liu, "SEED: Self-supervised distillation for visual representation," in *Proc. Int. Conf. Learn. Representations*, 2020.
- [9] S. Abbasi Koohpayegani, A. Tejankar, and H. Pirsiavash, "CompRes: Self-Supervised learning by compressing representations," *Proc. Int. Conf. Adv. Neural Info. Process. Syst.*, vol. 33, pp. 12980–12992, 2020.
- [10] H. M. Choi, H. Kang, and D. Oh, "Unsupervised representation transfer for small networks: I believe i can distill on-the-fly," in *Proc. Int. Conf. Adv. Neural Info. Process. Syst.*, 2021.
- [11] H. Bao, L. Dong, S. Piao, and F. Wei, "BEiT: BERT pre-training of image transformers," in *Proc. Int. Conf. Learn. Representations*, 2022.
- [12] K. He, X. Chen, S. Xie, Y. Li, P. Dollár, and R. B. Girshick, "Masked autoencoders are scalable vision learners," in *Proc. IEEE Conf. Comput. Vis. Pattern Recognit.*, 2022, pp. 15979–15988.

- [13] J. Zhou, C. Wei, H. Wang, W. Shen, C. Xie, A. Yuille, and T. Kong, "iBOT: Image bert pre-training with online tokenizer," in *Proc. Int. Conf. Learn. Representations*, 2022.
- [14] C. Ryali, Y.-T. Hu, D. Bolya, C. Wei, H. Fan, P.-Y. Huang, V. Aggarwal, A. Chowdhury, O. Poursaeed, J. Hoffman, J. Malik, Y. Li, and C. Feichtenhofer, "Hiera: A hierarchical vision transformer without the bells-and-whistles," in *Proc. Int. Conf. Mach. Learn.*, 2023, pp. 29 441–29 454.
- [15] A. Dosovitskiy, L. Beyer, A. Kolesnikov, D. Weissenborn, X. Zhai, T. Unterthiner, M. Dehghani, M. Minderer, G. Heigold, S. Gelly *et al.*, "An image is worth 16x16 words: Transformers for image recognition at scale," in *Proc. Int. Conf. Learn. Representations*, 2020.
- [16] H. Touvron, M. Cord, M. Douze, F. Massa, A. Sablayrolles, and H. Jegou, "Training data-efficient image transformers & distillation through attention," in *Proc. Int. Conf. Mach. Learn.*, vol. 139, 2021, pp. 10 347–10 357.
- [17] B. Graham, A. El-Nouby, H. Touvron, P. Stock, A. Joulin, H. Jégou, and M. Douze, "LeViT: A vision transformer in convnet's clothing for faster inference," in *Proc. Int. Conf. Comput. Vis.*, 2021, pp. 12 259–12 269.
- [18] A. Ali, H. Touvron, M. Caron, P. Bojanowski, M. Douze, A. Joulin, I. Laptev, N. Neverova, G. Synnaeve, J. Verbeek *et al.*, "Xcit: Cross-covariance image transformers," *Proc. Int. Conf. Adv. Neural Info. Process. Syst.*, vol. 34, 2021.
- [19] B. Heo, S. Yun, D. Han, S. Chun, J. Choe, and S. J. Oh, "Rethinking spatial dimensions of vision transformers," in *Proc. Int. Conf. Comput. Vis.*, 2021, pp. 11 936–11 945.
- [20] H. Touvron, M. Cord, A. Sablayrolles, G. Synnaeve, and H. Jégou, "Going deeper with image transformers," in *Proc. Int. Conf. Comput. Vis.*, 2021, pp. 32–42.
- [21] S. Mehta and M. Rastegari, "MobileViT: Light-weight, general-purpose, and mobile-friendly vision transformer," in *Proc. Int. Conf. Learn. Representations*, 2022.
- [22] Y. Chen, X. Dai, D. Chen, M. Liu, X. Dong, L. Yuan, and Z. Liu, "Mobile-Former: Bridging mobilenet and transformer," in *Proc. IEEE Conf. Comput. Vis. Pattern Recognit.*, 2022, pp. 5260–5269.
- [23] J. Pan, A. Bulat, F. Tan, X. Zhu, L. Dudziak, H. Li, G. Tzimiropoulos, and B. Martínez, "EdgeViTs: Competing light-weight cnns on mobile devices with vision transformers," in *Proc. Eur. Conf. Comput. Vis.*, 2022, pp. 294–311.
- [24] P. K. A. Vasu, J. Gabriel, J. Zhu, O. Tuzel, and A. Ranjan, "FastViT: A Fast Hybrid Vision Transformer using Structural Reparameterization," in *Proc. Int. Conf. Comput. Vis.*, 2023, pp. 5762–5772.
- [25] Y. Li, J. Hu, Y. Wen, G. Evangelidis, K. Salahi, Y. Wang, S. Tulyakov, and J. Ren, "Rethinking vision transformers for MobileNet size and speed," in *Proc. Int. Conf. Comput. Vis.*, 2023, pp. 16 843–16 854.
- [26] H. Cai, J. Li, M. Hu, C. Gan, and S. Han, "EfficientViT: Lightweight multi-scale attention for high-resolution dense prediction," in *Proc. Int. Conf. Comput. Vis.*, 2023, pp. 17 256–17 267.
- [27] Q. Wan, Z. Huang, J. Lu, G. Yu, and L. Zhang, "SeaFormer: Squeeze-enhanced axial transformer for mobile semantic segmentation," in *Proc. Int. Conf. Learn. Representations*, 2023.
- [28] Z. Xie, Z. Zhang, Y. Cao, Y. Lin, J. Bao, Z. Yao, Q. Dai, and H. Hu, "SimMIM: A simple framework for masked image modeling," in *Proc. IEEE Conf. Comput. Vis. Pattern Recognit.*, 2022.
- [29] A. van den Oord, O. Vinyals, and K. Kavukcuoglu, "Neural discrete representation learning," in *Proc. 31st Conf. Adv. Neural Info. Process. Syst.*, 2017.
- [30] A. Ramesh, M. Pavlov, G. Goh, S. Gray, C. Voss, A. Radford, M. Chen, and I. Sutskever, "Zero-shot text-to-image generation," in *Proc. Int. Conf. Mach. Learn.*, 2021, pp. 8821–8831.
- [31] X. Dong, J. Bao, T. Zhang, D. Chen, W. Zhang, L. Yuan, D. Chen, F. Wen, and N. Yu, "Bootstrapped masked autoencoders for vision BERT pretraining," in *Proc. Eur. Conf. Comput. Vis.*, 2022, pp. 247–264.
- [32] C. Wei, H. Fan, S. Xie, C. Wu, A. L. Yuille, and C. Feichtenhofer, "Masked feature prediction for self-supervised visual pre-training," in *Proc. IEEE Conf. Comput. Vis. Pattern Recognit.*, 2022, pp. 14 648–14 658.
- [33] S. Ren, F. Wei, Z. Zhang, and H. Hu, "TinyMIM: An empirical study of distilling MIM pre-trained models," in *Proc. IEEE Conf. Comput. Vis. Pattern Recognit.*, 2023, pp. 3687–3697.
- [34] S. Gidaris, P. Singh, and N. Komodakis, "Unsupervised representation learning by predicting image rotations," in *Proc. Int. Conf. Learn. Representations*, 2018.
- [35] R. Zhang, P. Isola, and A. A. Efros, "Colorful image colorization," in *Proc. Eur. Conf. Comput. Vis.*, 2016, pp. 649–666.
- [36] M. Noroozi and P. Favaro, "Unsupervised learning of visual representations by solving jigsaw puzzles," in *Proc. Eur. Conf. Comput. Vis.*, 2016, pp. 69–84.
- [37] A. Dosovitskiy, J. T. Springenberg, M. Riedmiller, and T. Brox, "Discriminative unsupervised feature learning with convolutional neural networks," *Proc. Int. Conf. Adv. Neural Info. Process. Syst.*, vol. 27, pp. 766–774, 2014.
- [38] D. Pathak, P. Krähenbühl, J. Donahue, T. Darrell, and A. A. Efros, "Context encoders: Feature learning by inpainting," in *Proc. IEEE Conf. Comput. Vis. Pattern Recognit.*, 2016, pp. 2536–2544.
- [39] Y. M. Asano, C. Rupprecht, and A. Vedaldi, "Self-labelling via simultaneous clustering and representation learning," in *Proc. Int. Conf. Learn. Representations*, 2020.
- [40] M. Caron, P. Bojanowski, A. Joulin, and M. Douze, "Deep clustering for unsupervised learning of visual features," in *Proc. Eur. Conf. Comput. Vis.*, 2018, pp. 139–156.
- [41] M. Caron, P. Bojanowski, J. Mairal, and A. Joulin, "Unsupervised pre-training of image features on non-curated data," in *Proc. Int. Conf. Comput. Vis.*, 2019, pp. 2959–2968.
- [42] J. Huang, Q. Dong, S. Gong, and X. Zhu, "Unsupervised deep learning by neighbourhood discovery," in *Proc. Int. Conf. Mach. Learn.*, 2019, pp. 2849–2858.
- [43] J. Li, P. Zhou, C. Xiong, and S. C. H. Hoi, "Prototypical contrastive learning of unsupervised representations," in *Proc. Int. Conf. Learn. Representations*, 2021.
- [44] J. Xie, R. B. Girshick, and A. Farhadi, "Unsupervised deep embedding for clustering analysis," in *Proc. Int. Conf. Mach. Learn.*, 2016, pp. 478–487.
- [45] J. Yang, D. Parikh, and D. Batra, "Joint unsupervised learning of deep representations and image clusters," in *Proc. IEEE Conf. Comput. Vis. Pattern Recognit.*, 2016, pp. 5147–5156.
- [46] C. Zhuang, A. L. Zhai, and D. Yamins, "Local aggregation for unsupervised learning of visual embeddings," in *Proc. Int. Conf. Comput. Vis.*, 2019, pp. 6001–6011.
- [47] T. Chen, S. Kornblith, M. Norouzi, and G. Hinton, "A simple framework for contrastive learning of visual representations," in *Proc. Int. Conf. Mach. Learn.* PMLR, 2020, pp. 1597–1607.
- [48] X. Chen and K. He, "Exploring simple siamese representation learning," in *Proc. IEEE Conf. Comput. Vis. Pattern Recognit.*, 2021, pp. 15 750–15 758.
- [49] A. Ermolov, A. Siarohin, E. Sangineto, and N. Sebe, "Whitening for self-supervised representation learning," in *Proc. Int. Conf. Mach. Learn.*, 2021, pp. 3015–3024.
- [50] J. Zbontar, L. Jing, I. Misra, Y. LeCun, and S. Deny, "Barlow twins: Self-supervised learning via redundancy reduction," in *Proc. Int. Conf. Mach. Learn.*, 2021, pp. 12 310–12 320.
- [51] S. Gidaris, A. Bursuc, N. Komodakis, P. Pérez, and M. Cord, "Learning representations by predicting bags of visual words," in *Proc. IEEE Conf. Comput. Vis. Pattern Recognit.*, 2020, pp. 6926–6936.
- [52] P. Bojanowski and A. Joulin, "Unsupervised learning by predicting noise," in *Proc. Int. Conf. Mach. Learn.*, 2017, pp. 517–526.
- [53] A. El-Nouby, G. Izacard, H. Touvron, I. Laptev, H. Jegou, and E. Grave, "Are large-scale datasets necessary for self-supervised pre-training?" *ArXiv*, vol. abs/2112.10740, 2021.
- [54] X. Chen, M. Ding, X. Wang, Y. Xin, S. Mo, Y. Wang, S. Han, P. Luo, G. Zeng, and J. Wang, "Context autoencoder for self-supervised representation learning," *International Journal of Computer Vision*, vol. 132, no. 1, pp. 208–223, 2024.
- [55] H. Wang, K. Song, J. Fan, Y. Wang, J. Xie, and Z. Zhang, "Hard patches mining for masked image modeling," in *Proc. IEEE Conf. Comput. Vis. Pattern Recognit.*, 2023, pp. 10 375–10 385.
- [56] I. Kakogeorgiou, S. Gidaris, B. Psomas, Y. Avrithis, A. Bursuc, K. Karantzalos, and N. Komodakis, "What to hide from your students: Attention-Guided masked image modeling," in *Proc. Eur. Conf. Comput. Vis.*, 2022, pp. 300–318.
- [57] Y. Shi, N. Siddharth, P. H. S. Torr, and A. R. Kosiorek, "Adversarial masking for self-supervised learning," in *Proc. Int. Conf. Mach. Learn.*, 2022, pp. 20 026–20 040.
- [58] G. Li, H. Zheng, D. Liu, C. Wang, B. Su, and C. Zheng, "SemMAE: Semantic-Guided masking for learning masked autoencoders," in *Proc. 36th Conf. Adv. Neural Info. Process. Syst.*, 2022.
- [59] X. Li, W. Wang, L. Yang, and J. Yang, "Uniform masking: Enabling MAE Pre-training for Pyramid-based Vision Transformers with Locality," *ArXiv*, vol. abs/2205.10063, 2022.
- [60] A. Baevski, W. Hsu, Q. Xu, A. Babu, J. Gu, and M. Auli, "data2vec: A General Framework for Self-supervised Learning in Speech," in *Proc. Int. Conf. Mach. Learn.*, 2022, pp. 1298–1312.
- [61] X. Dong, J. Bao, T. Zhang, D. Chen, W. Zhang, L. Yuan, D. Chen, F. Wen, N. Yu, and B. Guo, "PeCo: Perceptual Codebook for BERT

- Pre-training of Vision Transformers,” in *AAAI Conf. on Artificial Intelligence*, 2023, pp. 552–560.
- [62] Z. Hou, F. Sun, Y. Chen, Y. Xie, and S. Kung, “Milan: Masked Image Pretraining on Language Assisted Representation,” *ArXiv*, vol. abs/2208.06049, 2022.
- [63] J. D. M.-W. C. Kenton and L. K. Toutanova, “BERT: Pre-training of Deep Bidirectional Transformers for Language Understanding,” in *North American Chapter of the Association for Computational Linguistics*, 2019, pp. 4171–4186.
- [64] A. Radford, J. W. Kim, C. Hallacy, A. Ramesh, G. Goh, S. Agarwal, G. Sastry, A. Askell, P. Mishkin, J. Clark, G. Krueger, and I. Sutskever, “Learning transferable visual models from natural language supervision,” in *Proc. Int. Conf. Mach. Learn.*, 2021, pp. 8748–8763.
- [65] Z. Peng, L. Dong, H. Bao, Q. Ye, and F. Wei, “BEiTv2: Masked Image Modeling with Vector-Quantized Visual Tokenizers,” *ArXiv*, vol. abs/2208.06366, 2022.
- [66] S. Woo, S. Debnath, R. Hu, X. Chen, Z. Liu, I. S. Kweon, and S. Xie, “ConvNeXtV2: Co-designing and Scaling ConvNets with Masked Autoencoders,” in *Proc. IEEE Conf. Comput. Vis. Pattern Recognit.*, 2023, pp. 16 133–16 142.
- [67] P. Gao, T. Ma, H. Li, Z. Lin, J. Dai, and Y. Qiao, “MCMAE: Masked Convolution Meets Masked Autoencoders,” in *Proc. 36th Conf. Adv. Neural Info. Process. Syst.*, 2022.
- [68] A. Vaswani, N. Shazeer, N. Parmar, J. Uszkoreit, L. Jones, A. N. Gomez, L. Kaiser, and I. Polosukhin, “Attention is all you need,” *Proc. Int. Conf. Adv. Neural Info. Process. Syst.*, vol. 30, 2017.
- [69] S. Abnar, M. Dehghani, and W. Zuidema, “Transferring inductive biases through knowledge distillation,” *ArXiv*, vol. abs/2006.00555, 2020.
- [70] A. Steiner, A. Kolesnikov, X. Zhai, R. Wightman, J. Uszkoreit, and L. Beyer, “How to train your vit? data, augmentation, and regularization in vision transformers,” *Trans. Mach. Learn. Res.*, vol. 2022, 2022.
- [71] H. Touvron, M. Cord, and H. Jégou, “DeiT III: Revenge of the ViT,” in *Proc. Eur. Conf. Comput. Vis.*, 2022, pp. 516–533.
- [72] K. Simonyan and A. Zisserman, “Very deep convolutional networks for large-scale image recognition,” in *Proc. 3rd Int. Conf. Learn. Represent.*, May 2015.
- [73] C. Szegedy, V. Vanhoucke, S. Ioffe, J. Shlens, and Z. Wojna, “Rethinking the inception architecture for computer vision,” in *Proc. IEEE Conf. Comput. Vis. Pattern Recognit.*, 2016, pp. 2818–2826.
- [74] K. He, X. Zhang, S. Ren, and J. Sun, “Deep residual learning for image recognition,” in *Proc. IEEE Conf. Comput. Vis. Pattern Recognit.*, 2016, pp. 770–778.
- [75] G. Huang, Z. Liu, L. van der Maaten, and K. Q. Weinberger, “Densely connected convolutional networks,” in *Proc. IEEE Conf. Comput. Vis. Pattern Recognit.*, 2017, pp. 2261–2269.
- [76] M. Sandler, A. Howard, M. Zhu, A. Zhmoginov, and L.-C. Chen, “MobileNetV2: Inverted residuals and linear bottlenecks,” in *Proc. IEEE Conf. Comput. Vis. Pattern Recognit.*, 2018, pp. 4510–4520.
- [77] X. Zhang, X. Zhou, M. Lin, and J. Sun, “ShuffleNet: An extremely efficient convolutional neural network for mobile devices,” in *Proc. IEEE Conf. Comput. Vis. Pattern Recognit.*, 2018, pp. 6848–6856.
- [78] K. Han, Y. Wang, Q. Zhang, W. Zhang, C. Xu, and T. Zhang, “Model Rubik’s Cube: Twisting resolution, depth and width for TinyNets,” in *Proc. 34th Conf. Adv. Neural Info. Process. Syst.*, 2020.
- [79] I. Radosavovic, R. P. Kosaraju, R. Girshick, K. He, and P. Dollár, “Designing network design spaces,” in *Proc. IEEE Conf. Comput. Vis. Pattern Recognit.*, 2020, pp. 10 428–10 436.
- [80] Z. Liu, H. Mao, C.-Y. Wu, C. Feichtenhofer, T. Darrell, and S. Xie, “A convnet for the 2020s,” in *Proc. IEEE Conf. Comput. Vis. Pattern Recognit.*, 2022, pp. 11 966–11 976.
- [81] M. Tan and Q. Le, “Efficientnet: Rethinking model scaling for convolutional neural networks,” in *Proc. Int. Conf. Mach. Learn.*, 2019, pp. 6105–6114.
- [82] A. Howard, M. Sandler, G. Chu, L.-C. Chen, B. Chen, M. Tan, W. Wang, Y. Zhu, R. Pang, V. Vasudevan, Q. V. Le, and H. Adam, “Searching for MobileNetV3,” in *Proc. Int. Conf. Comput. Vis.*, 2019.
- [83] C. Liu, B. Zoph, M. Neumann, J. Shlens, W. Hua, L. Li, L. Fei-Fei, A. L. Yuille, J. Huang, and K. Murphy, “Progressive neural architecture search,” in *Proc. Eur. Conf. Comput. Vis.*, 2018, pp. 19–35.
- [84] H. Liu, K. Simonyan, and Y. Yang, “DARTS: Differentiable architecture search,” in *Proc. Int. Conf. Learn. Representations*, 2019.
- [85] H. Pham, M. Y. Guan, B. Zoph, Q. V. Le, and J. Dean, “Efficient neural architecture search via parameter sharing,” in *Proc. Int. Conf. Mach. Learn.*, 2018, pp. 4092–4101.
- [86] Z. Liu, Y. Lin, Y. Cao, H. Hu, Y. Wei, Z. Zhang, S. Lin, and B. Guo, “Swin transformer: Hierarchical vision transformer using shifted windows,” in *Proc. Int. Conf. Comput. Vis.*, 2021, pp. 10 012–10 022.
- [87] X. Dong, J. Bao, D. Chen, W. Zhang, N. Yu, L. Yuan, D. Chen, and B. Guo, “CSWin Transformer: A general vision transformer backbone with cross-shaped windows,” in *Proc. IEEE Conf. Comput. Vis. Pattern Recognit.*, 2022, pp. 12 114–12 124.
- [88] W. Wang, E. Xie, X. Li, D. Fan, K. Song, D. Liang, T. Lu, P. Luo, and L. Shao, “Pyramid Vision Transformer: A versatile backbone for dense prediction without convolutions,” in *Proc. Int. Conf. Comput. Vis.*, 2021, pp. 548–558.
- [89] L. Yuan, Y. Chen, T. Wang, W. Yu, Y. Shi, Z. Jiang, F. E. H. Tay, J. Feng, and S. Yan, “Tokens-to-Token ViT: Training vision transformers from scratch on imagenet,” in *Proc. Int. Conf. Comput. Vis.*, 2021, pp. 538–547.
- [90] A. Srinivas, T. Lin, N. Parmar, J. Shlens, P. Abbeel, and A. Vaswani, “Bottleneck transformers for visual recognition,” in *Proc. IEEE Conf. Comput. Vis. Pattern Recognit.*, 2021, pp. 16 519–16 529.
- [91] S. d’Ascoli, H. Touvron, M. L. Leavitt, A. S. Morcos, G. Biroli, and L. Sagun, “ConViT: Improving vision transformers with soft convolutional inductive biases,” in *Proc. Int. Conf. Mach. Learn.*, 2021, pp. 2286–2296.
- [92] S. Singh and A. Shrivastava, “CvT: Introducing convolutions to vision transformers,” in *Proc. Int. Conf. Comput. Vis.*, 2021, pp. 22–31.
- [93] W. Xu, Y. Xu, T. A. Chang, and Z. Tu, “Co-Scale conv-attentional image transformers,” in *Proc. Int. Conf. Comput. Vis.*, 2021, pp. 9961–9970.
- [94] T. Xiao, M. Singh, E. Mintun, T. Darrell, P. Dollár, and R. B. Girshick, “Early convolutions help transformers see better,” in *Proc. 35th Conf. Adv. Neural Info. Process. Syst.*, 2021.
- [95] S. Mehta and M. Rastegari, “Separable self-attention for mobile vision transformers,” in *Proc. Int. Conf. Learn. Representations*, 2023.
- [96] S. N. Wadkar and A. Chaurasia, “MobileViTv3: Mobile-Friendly vision transformer with simple and effective fusion of local, global and input features,” *ArXiv*, vol. abs/2209.15159, 2022.
- [97] M. Maaz, A. Shaker, H. Cholakkal, S. H. Khan, S. W. Zamir, R. M. Anwer, and F. S. Khan, “EdgeNeXt: Efficiently amalgamated cnn-transformer architecture for mobile vision applications,” in *Proc. Eur. Conf. Comput. Vis. Worksh.*, 2022, pp. 3–20.
- [98] S. Wang, J. Gao, Z. Li, X. Zhang, and W. Hu, “A closer look at self-supervised lightweight vision transformers,” in *Proc. Int. Conf. Mach. Learn.*, 2023.
- [99] C. Bucilua, R. Caruana, and A. Niculescu-Mizil, “Model compression,” in *Proc. ACM Int. Conf. on Knowledge Discovery and Data Mining*, 2006, pp. 535–541.
- [100] G. Hinton, O. Vinyals, and J. Dean, “Distilling the knowledge in a neural network,” *ArXiv*, vol. abs/1503.02531, 2015.
- [101] A. Romero, N. Ballas, S. E. Kahou, A. Chassang, C. Gatta, and Y. Bengio, “FitNets: Hints for thin deep nets,” in *Proc. Int. Conf. Learn. Representations*, 2015.
- [102] S. Zagoruyko and N. Komodakis, “Paying more attention to attention: Improving the performance of convolutional neural networks via attention transfer,” in *Proc. Int. Conf. Learn. Representations*, 2017.
- [103] W. Park, D. Kim, Y. Lu, and M. Cho, “Relational knowledge distillation,” in *Proc. IEEE Conf. Comput. Vis. Pattern Recognit.*, June 2019.
- [104] G. Chen, W. Choi, X. Yu, T. Han, and M. Chandraker, “Learning efficient object detection models with knowledge distillation,” *Proc. Int. Conf. Adv. Neural Info. Process. Syst.*, vol. 30, 2017.
- [105] T. He, C. Shen, Z. Tian, D. Gong, C. Sun, and Y. Yan, “Knowledge adaptation for efficient semantic segmentation,” in *Proc. IEEE Conf. Comput. Vis. Pattern Recognit.*, 2019, pp. 578–587.
- [106] V. Sanh, L. Debut, J. Chaumond, and T. Wolf, “DistilBERT, a distilled version of BERT: Smaller, faster, cheaper and lighter,” *ArXiv*, vol. abs/1910.01108, 2019.
- [107] X. Jiao, Y. Yin, L. Shang, X. Jiang, X. Chen, L. Li, F. Wang, and Q. Liu, “TinyBERT: Distilling bert for natural language understanding,” in *Findings of Empirical Methods in Natural Language Process.*, 2020, pp. 4163–4174.
- [108] W. Wang, H. Bao, S. Huang, L. Dong, and F. Wei, “MiniLMv2: Multi-Head self-attention relation distillation for compressing pretrained transformers,” in *Findings of Int. Joint Conf. on Natural Language Process.*, 2021, pp. 2140–2151.
- [109] Z. Sun, H. Yu, X. Song, R. Liu, Y. Yang, and D. Zhou, “MobileBERT: A Compact Task-Agnostic BERT For Resource-Limited Devices,” in *Association for Computational Linguistics*, 2020, pp. 2158–2170.

- [110] Y. Gao, J. Zhuang, S. Lin, H. Cheng, X. Sun, K. Li, and C. Shen, "DisCo: Remediating self-supervised learning on lightweight models with distilled contrastive learning," in *Proc. Eur. Conf. Comput. Vis.*, 2022, pp. 237–253.
- [111] Y. Wei, H. Hu, Z. Xie, Z. Zhang, Y. Cao, J. Bao, D. Chen, and B. Guo, "Contrastive learning rivals masked image modeling in fine-tuning via feature distillation," *ArXiv*, vol. abs/2205.14141, 2022.
- [112] C. Li, J. Yang, P. Zhang, M. Gao, B. Xiao, X. Dai, L. Yuan, and J. Gao, "Efficient self-supervised vision transformers for representation learning," in *Proc. Int. Conf. Learn. Representations*, 2022.
- [113] P. Bhat, E. Arani, and B. Zonooz, "Distill on the Go: Online knowledge distillation in self-supervised learning," in *Proc. IEEE Conf. Comput. Vis. Pattern Recognit.*, 2021, pp. 2678–2687.
- [114] Y. Tian, D. Krishnan, and P. Isola, "Contrastive representation distillation," in *Proc. Int. Conf. Learn. Representations*, 2019.
- [115] G. Xu, Z. Liu, X. Li, and C. C. Loy, "Knowledge distillation meets self-supervision," in *Proc. Eur. Conf. Comput. Vis.* Springer, 2020, pp. 588–604.
- [116] C. Raffel, N. Shazeer, A. Roberts, K. Lee, S. Narang, M. Matena, Y. Zhou, W. Li, and P. J. Liu, "Exploring the limits of transfer learning with a unified text-to-text transformer," *The Journal of Machine Learning Research*, vol. 21, pp. 140:1–140:67, 2020.
- [117] H. Bao, L. Dong, F. Wei, W. Wang, N. Yang, X. Liu, Y. Wang, J. Gao, S. Piao, M. Zhou, and H. Hon, "UniLMv2: Pseudo-Masked language models for unified language model pre-training," in *Proc. Int. Conf. Mach. Learn.*, 2020, pp. 642–652.
- [118] H. Hu, J. Gu, Z. Zhang, J. Dai, and Y. Wei, "Relation networks for object detection," in *Proc. IEEE Conf. Comput. Vis. Pattern Recognit.*, 2018, pp. 3588–3597.
- [119] H. Hu, Z. Zhang, Z. Xie, and S. Lin, "Local relation networks for image recognition," in *Proc. IEEE Conf. Comput. Vis. Pattern Recognit.*, 2019, pp. 3463–3472.
- [120] P. Shaw, J. Uszkoreit, and A. Vaswani, "Self-attention with relative position representations," in *North American Chapter of the Association for Computational Linguistics*, 2018, pp. 464–468.
- [121] A. Newell and J. Deng, "How useful is self-supervised pretraining for visual tasks?" in *Proc. IEEE Conf. Comput. Vis. Pattern Recognit.*, 2020, pp. 7345–7354.
- [122] X. Chu, Z. Tian, B. Zhang, X. Wang, and C. Shen, "Conditional positional encodings for vision transformers," in *Proc. Int. Conf. Learn. Representations*, 2023.
- [123] M. Assran, M. Caron, I. Misra, P. Bojanowski, A. Joulin, N. Ballas, and M. Rabbat, "Semi-supervised learning of visual features by non-parametrically predicting view assignments with support samples," in *Proc. Int. Conf. Comput. Vis.*, 2021, pp. 8443–8452.
- [124] Z. Liu, Z. Miao, X. Zhan, J. Wang, B. Gong, and S. X. Yu, "Large-scale long-tailed recognition in an open world," in *Proc. IEEE Conf. Comput. Vis. Pattern Recognit.*, 2019.
- [125] M.-E. Nilsback and A. Zisserman, "Automated flower classification over a large number of classes," in *Indian Conference on Computer Vision, Graphics & Image Processing*, 2008, pp. 722–729.
- [126] O. M. Parkhi, A. Vedaldi, A. Zisserman, and C. V. Jawahar, "Cats and dogs," in *Proc. IEEE Conf. Comput. Vis. Pattern Recognit.*, 2012, pp. 3498–3505.
- [127] S. Maji, E. Rahtu, J. Kannala, M. Blaschko, and A. Vedaldi, "Fine-grained visual classification of aircraft," *ArXiv*, vol. abs/1306.5151, 2013.
- [128] J. Krause, M. Stark, J. Deng, and L. Fei-Fei, "3d object representations for fine-grained categorization," in *Int. Conf. Comput. Vis. Worksh.*, 2013, pp. 554–561.
- [129] A. Krizhevsky *et al.*, "Learning multiple layers of features from tiny images," *Technical Report*, 2009.
- [130] G. Van Horn, O. Mac Aodha, Y. Song, Y. Cui, C. Sun, A. Shepard, H. Adam, P. Perona, and S. Belongie, "The inaturalist species classification and detection dataset," in *Proc. IEEE Conf. Comput. Vis. Pattern Recognit.*, 2018.
- [131] G. Huang, Y. Sun, Z. Liu, D. Sedra, and K. Q. Weinberger, "Deep networks with stochastic depth," in *Proc. Eur. Conf. Comput. Vis.*, 2016, pp. 646–661.
- [132] T. Lin, M. Maire, S. J. Belongie, J. Hays, P. Perona, D. Ramanan, P. Dollár, and C. L. Zitnick, "Microsoft COCO: Common objects in context," in *Proc. Eur. Conf. Comput. Vis.*, 2014, pp. 740–755.
- [133] B. Zhou, H. Zhao, X. Puig, S. Fidler, A. Barriuso, and A. Torralba, "Scene parsing through ADE20K dataset," in *Proc. IEEE Conf. Comput. Vis. Pattern Recognit.*, 2017, pp. 5122–5130.
- [134] H. Fan, L. Lin, F. Yang, P. Chu, G. Deng, S. Yu, H. Bai, Y. Xu, C. Liao, and H. Ling, "LaSOT: A high-quality benchmark for large-scale single object tracking," in *Proc. IEEE Conf. Comput. Vis. Pattern Recognit.*, 2019, pp. 5369–5378.
- [135] Y. Li, S. Xie, X. Chen, P. Dollar, K. He, and R. Girshick, "Benchmarking detection transfer learning with vision transformers," *ArXiv*, vol. abs/2111.11429, 2021.
- [136] T. Xiao, Y. Liu, B. Zhou, Y. Jiang, and J. Sun, "Unified perceptual parsing for scene understanding," in *Proc. Eur. Conf. Comput. Vis.*, 2018, pp. 432–448.
- [137] B. Ye, H. Chang, B. Ma, S. Shan, and X. Chen, "Joint feature learning and relation modeling for tracking: A one-stream framework," in *Proc. Eur. Conf. Comput. Vis.*, 2022, pp. 341–357.
- [138] C. Cortes, M. Mohri, and A. Rostamizadeh, "Algorithms for learning kernels based on centered alignment," *The Journal of Machine Learning Research*, vol. 13, pp. 795–828, 2012.
- [139] T. Nguyen, M. Raghu, and S. Kornblith, "Do wide and deep networks learn the same things? uncovering how neural network representations vary with width and depth," in *Proc. Int. Conf. Learn. Representations*, 2020.
- [140] L. Song, A. Smola, A. Gretton, J. Bedo, and K. Borgwardt, "Feature selection via dependence maximization," *The Journal of Machine Learning Research*, vol. 13, no. 5, 2012.
- [141] J. L. Ba, J. R. Kiros, and G. E. Hinton, "Layer normalization," *ArXiv*, vol. abs/1607.06450, 2016.
- [142] H. Fan, B. Xiong, K. Mangalam, Y. Li, Z. Yan, J. Malik, and C. Feichtenhofer, "Multiscale vision transformers," in *Proc. Int. Conf. Comput. Vis.*, 2021, pp. 6804–6815.
- [143] Y. Li, C. Wu, H. Fan, K. Mangalam, B. Xiong, J. Malik, and C. Feichtenhofer, "MViTv2: Improved multiscale vision transformers for classification and detection," in *Proc. IEEE Conf. Comput. Vis. Pattern Recognit.*, 2022, pp. 4794–4804.
- [144] L. Beyer, X. Zhai, A. Royer, L. Markeeva, R. Anil, and A. Kolesnikov, "Knowledge distillation: A good teacher is patient and consistent," in *Proc. IEEE Conf. Comput. Vis. Pattern Recognit.*, 2022, pp. 10915–10924.
- [145] X. Liu, H. Peng, N. Zheng, Y. Yang, H. Hu, and Y. Yuan, "EfficientViT: Memory efficient vision transformer with cascaded group attention," in *Proc. IEEE Conf. Comput. Vis. Pattern Recognit.*, 2023, pp. 14420–14430.
- [146] T. Huang, L. Huang, S. You, F. Wang, C. Qian, and C. Xu, "LightViT: Towards light-weight convolution-free vision transformers," *ArXiv*, vol. abs/2207.05557, 2022.
- [147] B. Kang, X. Chen, D. Wang, H. Peng, and H. Lu, "Exploring lightweight hierarchical vision transformers for efficient visual tracking," in *Proc. Int. Conf. Comput. Vis.*, 2023, pp. 9578–9587.
- [148] B. Yan, H. Peng, K. Wu, D. Wang, J. Fu, and H. Lu, "LightTrack: Finding lightweight neural networks for object tracking via one-shot architecture search," in *Proc. IEEE Conf. Comput. Vis. Pattern Recognit.*, 2021, pp. 15180–15189.
- [149] P. Blatter, M. Kanakis, M. Danelljan, and L. V. Gool, "Efficient visual tracking with exemplar transformers," in *IEEE Conf. on Applications Comput. Vis.*, 2023, pp. 1571–1581.
- [150] V. Borsuk, R. Vei, O. Kupyn, T. Martyniuk, I. Krashenyi, and J. Matas, "FEAR: Fast, efficient, accurate and robust visual tracker," in *Proc. Eur. Conf. Comput. Vis.*, 2022, pp. 644–663.
- [151] X. Chen, B. Kang, D. Li, and H. Lu, "Efficient visual tracking via hierarchical cross-attention transformer," in *Proc. Eur. Conf. Comput. Vis. Worksh.*, 2022, pp. 461–477.
- [152] Y. Cui, T. Song, G. Wu, and L. Wang, "MixFormerV2: Efficient fully transformer tracking," in *Proc. 37th Conf. Adv. Neural Info. Process. Syst.*, 2023.
- [153] A. Kirillov, R. B. Girshick, K. He, and P. Dollár, "Panoptic feature pyramid networks," in *Proc. IEEE Conf. Comput. Vis. Pattern Recognit.*, 2019, pp. 6399–6408.
- [154] P. Goyal, P. Dollár, R. Girshick, P. Noordhuis, L. Wesolowski, A. Kyrola, A. Tulloch, Y. Jia, and K. He, "Accurate, large minibatch sgd: Training imagenet in 1 hour," *ArXiv*, vol. abs/1706.02677, 2017.
- [155] I. Loshchilov and F. Hutter, "SGDR: Stochastic gradient descent with warm restarts," in *Proc. Int. Conf. Learn. Representations*, 2017.
- [156] E. D. Cubuk, B. Zoph, J. Shlens, and Q. Le, "RandAugment: Practical automated data augmentation with a reduced search space," in *Proc. Int. Conf. Adv. Neural Info. Process. Syst.*, vol. 33, 2020, pp. 18613–18624.
- [157] H. Zhang, M. Cisse, Y. N. Dauphin, and D. Lopez-Paz, "mixup: Beyond empirical risk minimization," in *Proc. Int. Conf. Learn. Representations*, 2018.
- [158] S. Yun, D. Han, S. J. Oh, S. Chun, J. Choe, and Y. Yoo, "Cutmix: Regularization strategy to train strong classifiers with localizable features," in *Proc. Int. Conf. Comput. Vis.*, 2019, pp. 6023–6032.

Supplementary Material

This is a supplementary material for our paper “Observation, Analysis, and Solution: Exploring Strong Lightweight Vision Transformers via Masked Image Modeling Pre-Training”.

APPENDIX A EXPERIMENTAL DETAILS

A.1 Recipe for Supervised Training of ViT-Tiny on IN1K

We largely follow the common practice of supervised ViT training in [16] except for some optimized hyperparameters for augmentations (*i.e.*, weaker regularization and augmentation than training large-scale models). The setting is detailed in Tab. S1. We use the linear learning rate (*lr*) scaling rule [154]: $lr = \text{base } lr \times \text{batch size} / 256$. We use layer-wise *lr* decay following [11], [12].

TABLE S1
Details of the Recipe for Supervised Training of ViT-Tiny on IN1K.

Config.	Value
optimizer	AdamW
base <i>lr</i>	1e-3
weight decay	0.05
optimizer momentum	$\beta_1, \beta_2 = 0.9, 0.999$
batch size	1024
<i>lr</i> schedule	cosine decay [155]
warmup epochs	5
training epochs	300
augmentation	RandAug(10, 0.5) [156]
colorjitter	0.3
label smoothing	0
mixup [157]	0.2
cutmix [158]	0
drop path [131]	0

A.2 Transfer Evaluation Details for Classification Tasks

We use 6 relatively smaller datasets than IN1K for transfer learning evaluation: Flowers [125], Pets [126], Aircraft [127], Cars [128], Cifar100 [129], and iNat18 [130]. For all these datasets except iNat18, we fine-tune with SGD (momentum=0.9), and the batch size is set to 512. The learning rates are swept over 3 candidates and the training epochs are swept over 2 candidates per dataset as detailed in Tab. S2. We adopt the cosine decay learning rate schedule [155] with a linear warm-up. We resize images to 224×224 . We adopt random resized crop and random horizontal flipping as augmentations and do not use any regularization (*e.g.*, weight decay, dropout, or the stochastic depth regularization technique [131]). For iNat18, we follow the same training configurations as those on IN1K.

TABLE S2
Transfer Evaluation Details for Some Downstream Classification Tasks.

Datasets	Learning rate	#Epochs (total, warm-up)	Layer-wise <i>lr</i> decay
Flowers	{0.01, 0.03, 0.1}	{(150,30), (250,50)}	{1.0, 0.75}
Pets	{0.01, 0.03, 0.1}	{(70,14), (150,30)}	{1.0, 0.75}
Aircraft	{0.01, 0.03, 0.1}	{(50,10), (100,20)}	{1.0, 0.75}
Cars	{0.01, 0.03, 0.1}	{(50,10), (100,20)}	{1.0, 0.75}
CIFAR100	{0.03, 0.1, 0.3}	{(25, 5), (50,10)}	{1.0, 0.75}

APPENDIX B MORE ANALYSES ON THE PRE-TRAINING

B.1 Analyses with More Models as Reference

In the main paper, the analyses based on the layer-wise representation similarity are mainly conducted by adopting the fully-supervised ViT-Tiny trained on the IN1K classification task based on our recipe (see Tab. 1) as the reference model. Here, we additionally introduce stronger recognition models as references to demonstrate the generalizability of our analyses. Specifically, we use ViT-Base models trained with various recipes as references, *e.g.*, DeiT-Base (supervised training on IN1K following [16] which achieves 82.0% top-1 accuracy on IN1K), ViT-Base-21k (supervised pre-training on IN21K following [70]), ViT-Base-21k-1k (first supervised pre-training on IN21K and then fine-tuning on IN1K following [70], achieving 84.5% top-1 accuracy on IN1K). The layer representation similarity is presented in Fig. S1.

First, we observe that our used reference model in the main paper is aligned well with these larger models (as shown in the left column of Fig. S1). We conjecture that the supervised training generally makes the vanilla ViT models have similar layer representation structures. Based on these stronger reference models, we observe similar phenomena for MAE pre-training and MoCo-v3 pre-training of ViT-Tiny as discussed in the main paper, which demonstrates the robustness of our analyses and conclusions w.r.t. different reference models.

Then, we analyze the larger MAE pre-trained ViT-Base with these newly introduced models as references, as shown in the last column of Fig. S1. We observe that MAE pre-trained ViT-Base still aligns relatively well with these much stronger recognition models, which supports our claim in the main paper that *it is possible to extract features relevant to recognition in higher layers for the up-scaled encoder in MAE pre-training*. It is the prerequisite for the improvement of the pre-trained ViT-Tiny based on the proposed distillation.

APPENDIX C MORE ANALYSES ON DISTILLATION

C.1 Applying Distillation on More Networks

To further evaluate our proposed distillation method, we additionally apply D-MAE to the pre-training of ViT-Small beyond ViT-Tiny using the MAE pre-trained ViT-Base as the teacher. The configurations of these models are presented in Tab. S3. The transfer evaluation results are presented in Tab. S4. The transfer performance of the pre-trained ViT-Small based on D-MAE surpasses the baseline model without distillation during pre-training by a large margin, which shows the efficacy of the distillation following our observation-analysis-solution flow.

TABLE S3
Configurations of Vanilla ViTs.

Models	Channel Dimension	#Heads	#Layers	#Params
ViT-Tiny	192	12	12	6M
ViT-Small	384	12	12	22M
ViT-Base	768	12	12	86M

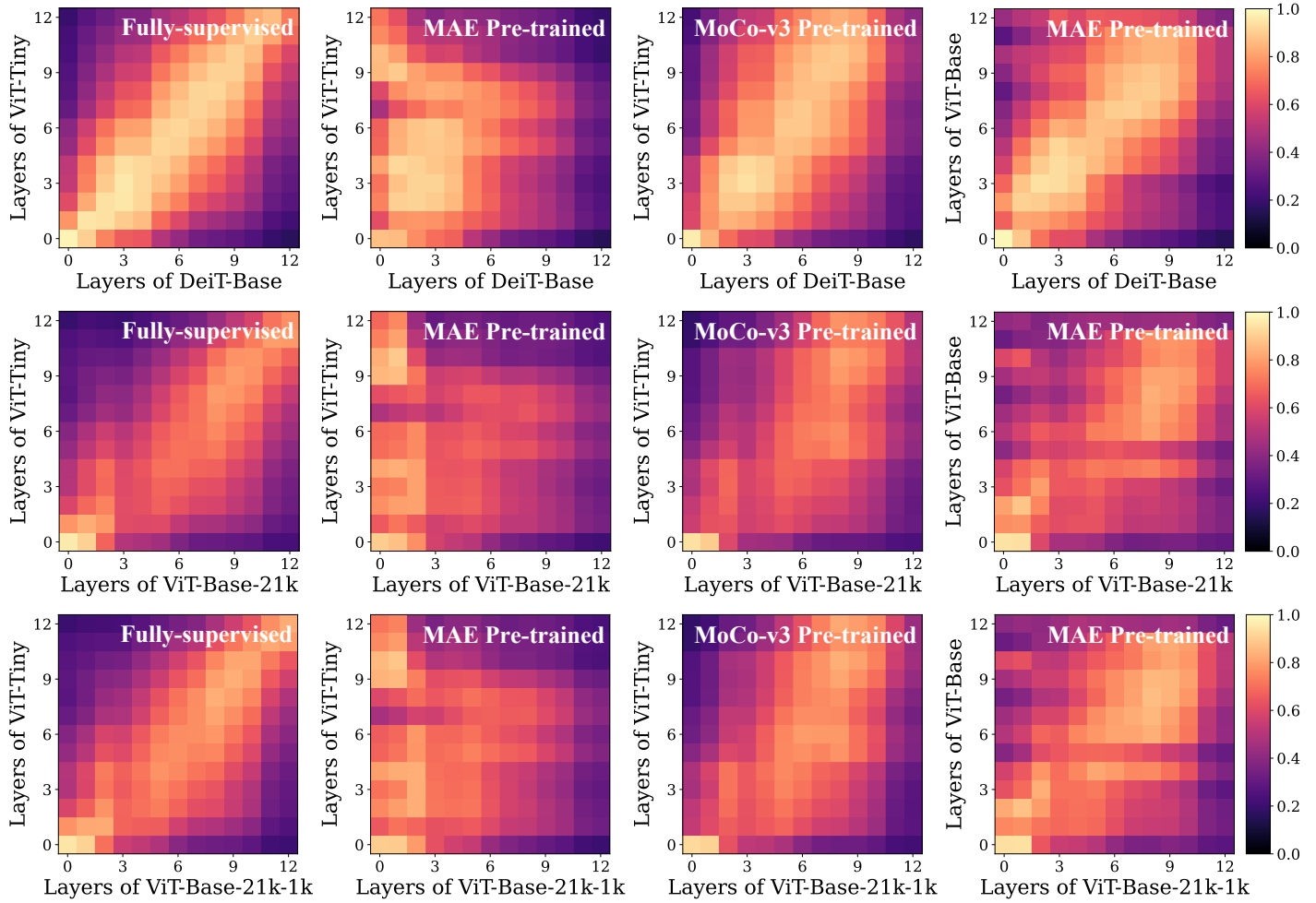


Fig. S1. **Layer representation analyses** with DeiT-Base (supervised training on IN1K following [16] which achieves 82.0% top-1 accuracy on IN1K), ViT-Base-21k (supervised pre-training on IN21K following [70]), ViT-Base-21k-1k (first supervised pre-training on IN21K and then fine-tuning on IN1K following [70], achieving 84.5% top-1 accuracy on IN1K) as the reference models.

TABLE S4

Applying D-MAE to the Pre-Training of ViT-Small. Top-1 Accuracy for the Transfer Performance on Downstream Classification Tasks of Pre-Trained Models W/ or W/O Distillation Is Reported.

Methods	Datasets						
	Flowers	Pets	Aircraft	Cars	CIFAR100	iNat18	IN1K
<i>Supervised (IN1K)</i>							
Our Recipe	97.4	94.2	77.6	88.2	89.2	66.5	80.2
<i>Self-Supervised</i>							
MAE	91.2	82.0	65.8	79.2	80.8	63.2	82.1
D-MAE	95.8	91.4	80.7	88.3	87.8	66.9	82.5
Δ to MAE	+4.6	+9.4	+14.9	+9.1	+7.0	+3.7	+0.4